

SOLVENT VISCOSITY AND PROTEIN DYNAMICS

by

MICHAEL C. MARDEN

B.S., University of Missouri, 1974

M.S., University of Illinois, 1976

THESIS

Submitted in partial fulfillment of the requirements  
for the degree of Doctor of Philosophy in Physics  
in the Graduate College of the  
University of Illinois at Urbana-Champaign, 1981

Urbana, Illinois

## ACKNOWLEDGEMENTS

I would like to thank my advisor, Hans Frauenfelder, for his "dynamic" guidance and teaching of physics. I especially appreciate his encouragement of a balance of culture, athletics, and science.

I was fortunate to have the advice of a growing physics faculty who are interested in biomolecules: Peter Debrunner, Giovanni DePasquali, Laura Eisenstein, Enrico Gratton, and Mike Weissman.

I would also like to thank my coworkers for their help and friendship: Niel Alberding, Dave Good, Peter Hänggi, Chris Hardy, Jeff Marque, Pál Ormos, Al Reynolds, and Kwok To Yue. A special thanks goes to Dan Beece for his computer graphics magic, and to Wolfgang Doster for helping with the "Internal viscosity" section. An extra-curricular thanks goes to Callahan, Granfors, Kolbas, and the Koos. Finally, a blue thank you to the members of the night shift who devoted much time and thought for this research: Lou Reinisch and Larry Sorensen.

This work was supported in part by the U.S. Department of Health, Education, and Welfare (Grant GM-18051) and by the National Science Foundation under Grants PCM-76-81025 and INT-78-26706.

## TABLE OF CONTENTS

	page
I. INTRODUCTION .....	1
A. Background on myoglobin .....	1
B. Analysis .....	3
II. EXPERIMENTAL .....	6
A. Flash photolysis .....	6
B. Sample preparation .....	6
C. Solubility measurements .....	10
D. Diffusivity measurements .....	13
III. RESULTS .....	14
A. Kinetics of Mb-CO and Mb-O <sub>2</sub> .....	14
B. Results in various solvents .....	14
C. Errors in measurements .....	25
IV. ANALYSIS .....	27
A. Reaction rate theory .....	27
B. Multiple process kinetics .....	29
C. Error analysis .....	40
D. Tables .....	42
V. INTERPRETATION .....	44
A. Fluctuating protein model .....	44
B. Internal viscosity .....	51
Appendix	
A. Diffusion .....	54
B. Nonexponential kinetics .....	70
C. Other proteins .....	72
REFERENCES .....	82
VITA .....	84

## I. INTRODUCTION

### A. Background on myoglobin

A single biomolecule is a complex object. While some may be designed only for geometrical reasons (lock and key model), others seem to require some internal motion to perform their function. A dioxygen molecule ( $O_2$ ) must penetrate a myoglobin molecule (Mb, figure 1) by at least six angstroms (Å) to bind at the buried iron atom. The binding would not be possible if the protein were rigid and not subject to fluctuations large enough to permit passage of the ligand (Case and Karplus, 1979; Alberding et al, 1978). Recent x-ray crystallography work has revealed the mean square displacement of all the atoms in the Mb molecule (Frauenfelder, Petsko, and Tsernoglou, 1979; figure 2). These motions and larger coordinated oscillations play an important role in the binding process. Such dynamic systems as Mb should be influenced by the viscoelastic properties of their environment. Specifically the binding of  $O_2$  and CO to Mb has been studied as a function of temperature (T) and solvent viscosity ( $\eta$ ). Since high viscosity will damp out certain oscillations, the viscosity dependence of the rates through the protein channel will provide information about the protein motion and how the biomolecule is coupled to its environment.

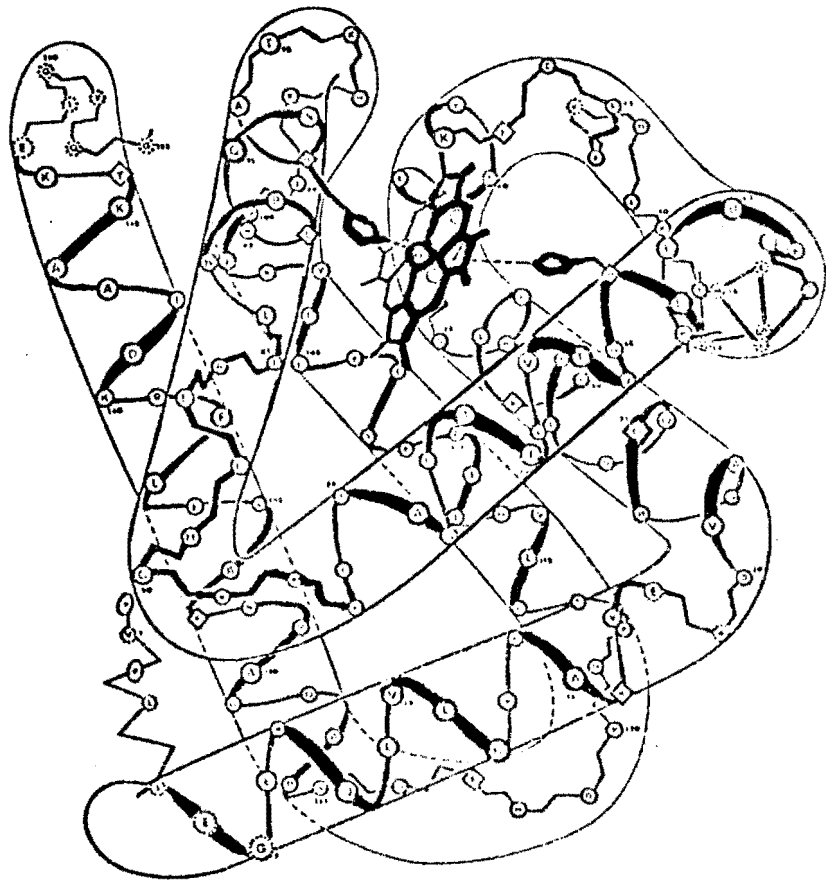
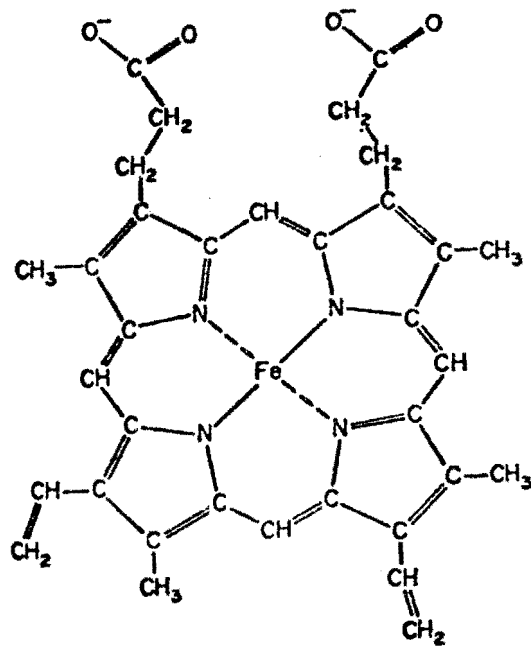


Figure 1  
 top: Fe-protoporphyrin-IX (protoheme), a planar organic molecule which binds CO reversibly, but is oxidized by oxygen.  
 bottom: Backbone of myoglobin (Mb; Dickerson, 1964).

Mb is responsible in mammals for the storage and distribution of oxygen. Mb is found mainly in the muscle cells where O<sub>2</sub> is used in an energy releasing reaction. This protein of MW 17,000 consists of an active site, Fe-protoporphyrin IX (protoheme), surrounded by a globular protein structure about 30Å in diameter (figure 1). The protein structure is a linear sequence of amino acids which fold to a unique shape (except for fluctuations). The protein structure prevents the oxidation of the iron atom allowing for reversible O<sub>2</sub> binding. However, it must also adjust the rates for the O<sub>2</sub> to come on or off so that the Mb takes up or releases oxygen as the biological system requires. Different species may have several substitutions within the sequence of amino acids; however, certain positions are invariant and the overall structure of the protein does not change substantially. Thus, the protein structure is not simply a box, but the 153 amino acids were carefully chosen to perform a specific function.

## B. Analysis

The measurements presented in this work are recombination kinetics after photodissociation of protein-ligand systems. The usual analysis is to fit the rates to the Arrhenius form  $k=A \exp(-H/RT)$ , with constant A and H, R being the gas constant (8.31 J/mole K). This form describes the temperature dependence of the rate for reactants attempting to overcome a

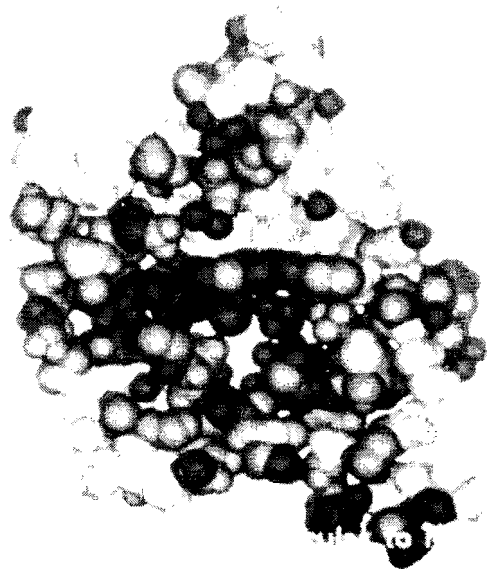


Figure 2

A 3A slice of Mb, perpendicular to the heme plane. The darker regions represent less motion. The small gaps between atoms show that some motion is required for the ligand to penetrate the protein.

barrier of height  $H$ . Although this simple analysis has been successful in fitting much kinetic data, it does not take into account the solvent viscosity.

Kramers has described the crossing of a barrier as a Brownian motion in a viscous medium (Kramers, 1940). He obtained the form  $k \propto (w w' / \eta) \exp(-H/RT)$  in the high viscosity limit.  $w$  is the oscillator frequency at the bottom of the well.  $w'$  the frequency at the top of the barrier (an inverted well). The present data can be fit to this form if  $\eta$  is replaced with  $\eta^k$ ,  $0 < k < 1$ . This behavior shall be discussed in terms of an effective or internal viscosity which is shielded from the solvent viscosity.

A diffusion model also has a  $1/\eta$  dependence describing a reaction limited by the collision frequency of the reactants. A diffusion model should be considered before one can draw conclusions about the barriers. If the rates were simply the collision frequency, then the rates would be controlled by the solvent and discussion of protein barriers would not be important. The observed kinetics can be fit with a series of barriers. Only the slowest process depends on the ligand concentration and is a candidate for a diffusion model. This model will be discussed in Appendix A.



## II. EXPERIMENTAL

### A. Flash photolysis

There is a large change in the visible absorption spectrum of Mb (figure 3) when the ligand is dissociated. By measuring the transmitted light at a wavelength where the change is large, 425nm for protoheme and 436nm for the proteins, one can determine the fraction of the sample in the bound state. The photomultiplier (RCA 4837) is designed to be free of hysteresis to allow for detection of rapid changes in light intensity. The signal is recorded by a transient digitizer (Tektronix 7912) and a logarithmic transient recorder (Austin et al 1976). These devices are interfaced to a minicomputer (Data General Nova 2) to provide on-line analysis and plotting (HP graphics terminal). A lus dye laser at 540nm or a 30ns neodymium glass laser pulse at 530nm is used to dissociate the molecules (figure 4).

### B. Sample preparation

Mixtures of water with glycerol, ethylene glycol, sucrose, and methanol were used to vary the viscosity (Miner and Dalton, 1953; Curme, 1952; Douzou, 1976). Results in methanol are mainly for protoheme-CO, since Mb denatures in mixtures of more than 50% methanol. The glycerol stock was stored under an atmosphere of CO or argon to prevent the

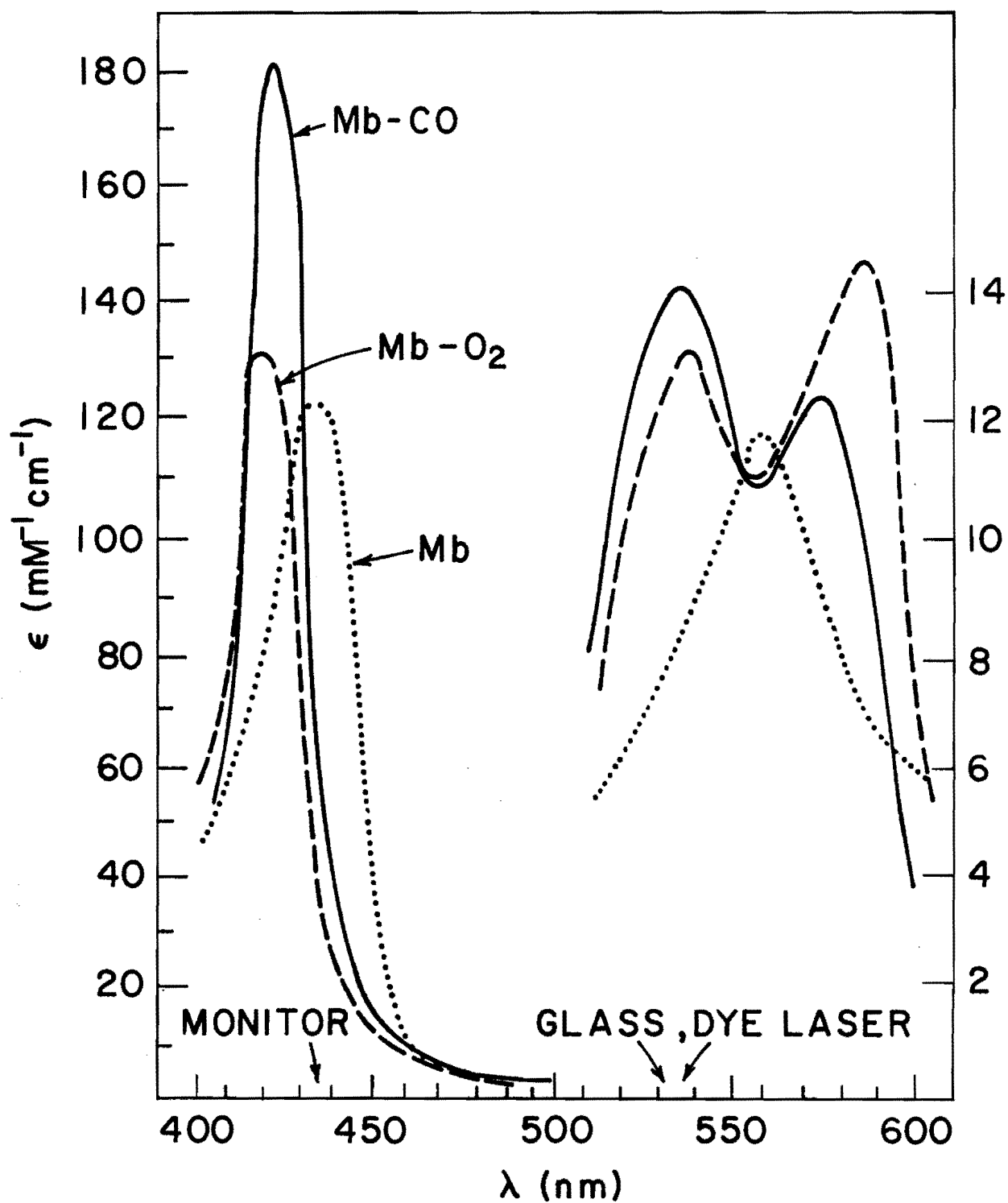
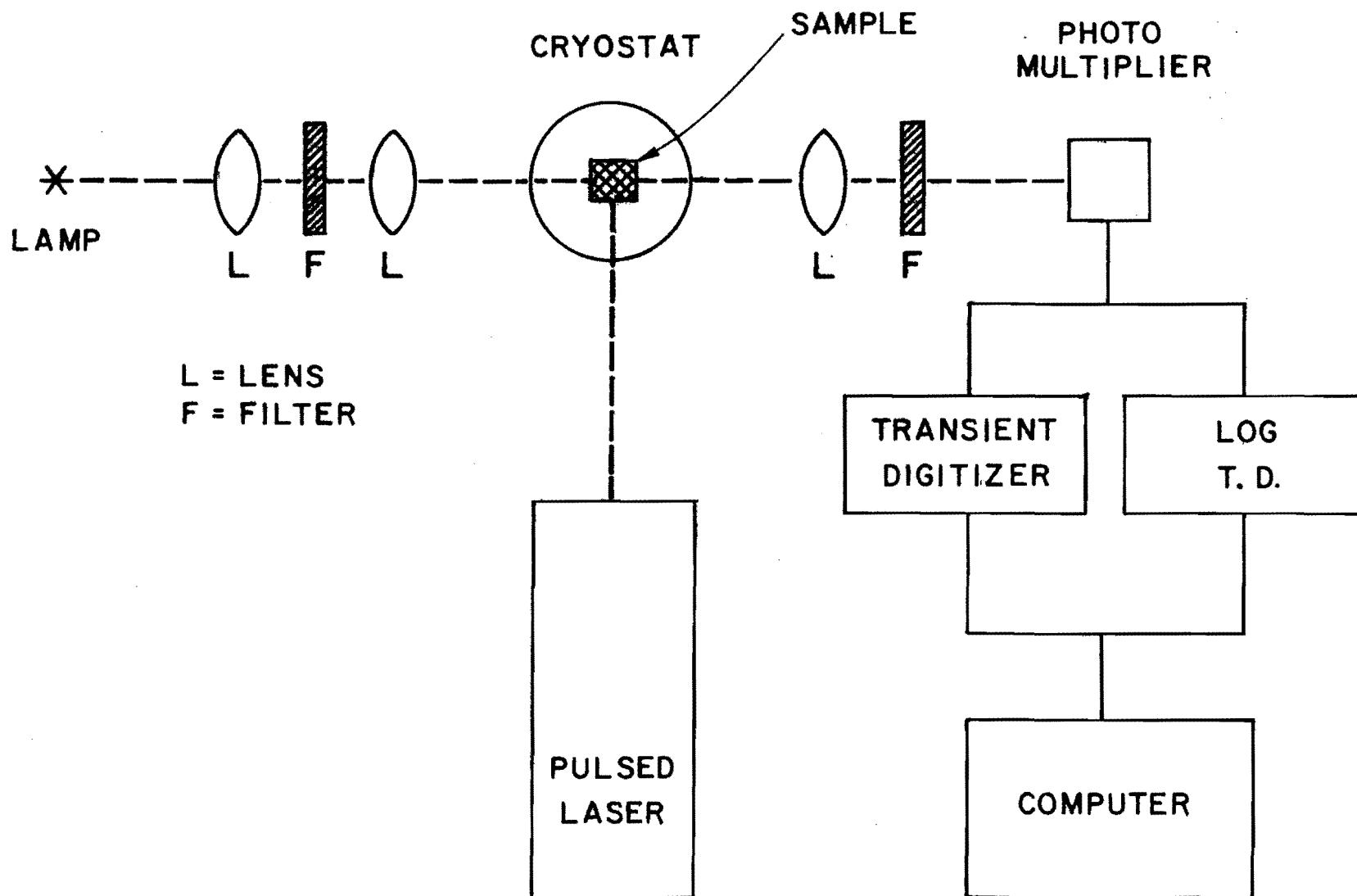


Figure 3  
Visible spectra of Mb, Mb-CO, and Mb-O<sub>2</sub>. The reaction is monitored at 436nm. The photolysing laser pulse is at 530nm or 540nm which is absorbed by the porphyrin ring.

Figure 4

Experimental schematic:

- A. Laser pulse: .6 us (FWHM) at 530nm - Phase R dye laser  
or 30 ns (FWHM) at 540nm - neodymium glass laser.  
energy=.2 J which is about  $10^{17}$  photons/pulse
- B. Monitoring light: 150W quartz iodine lamp  
filters (DITRIC 3-cavity), 7nm(FWHM) at 436nm for Mb  
intensity at 436nm -  $10^{14}$  photons/second.
- C. Photomultiplier tube - RCA 4837 (antihysteresis)  
Transient digitizer - 400 MHz Tektronix 7912  
Log trans. digitizer - Homebuilt with 1 MHz log time base  
Computer - Data General Nova 2
- D. Sample: Stock obtained from Sigma Inc.  
10uM samples in a 1cm cuvette.  
monitored volume -  $0.5\text{cm}^2$  by 1cm -  $3 \times 10^{15}$  molecules.



uptake of water. Samples consisted of 10uM protein (Sigma Inc.) and 50mM phosphate buffer, pH=7 in water, in the selected solvent in a 1cm cuvette. Samples were reduced with an excess of dithionite 2:1, for Mb-O2 and 10:1 for CO samples. The region of temperature and viscosity of interest is shown in figure 5.

### C. Solubility measurements

The rate of the slowest process is proportional to the ligand concentration [L]; therefore, [L] is needed to calculate the second order rate coefficient. Only limited data are available for the solubility and diffusivity of the ligands in glycerol (Seidell, 1940; Ackerman and Berger, 1963). Additional measurements of the solubility were made by the following method. The reaction  $\text{Mb} + \text{L} \rightarrow \text{Mb-L}$  (bound state) is second order at room temperature, satisfying the differential equation  $d[\text{Mb-L}]/dt = \lambda'[\text{Mb}][\text{L}]$ . When there is a large excess of one reactant, the reaction becomes psuedo first order, with the observed rate :

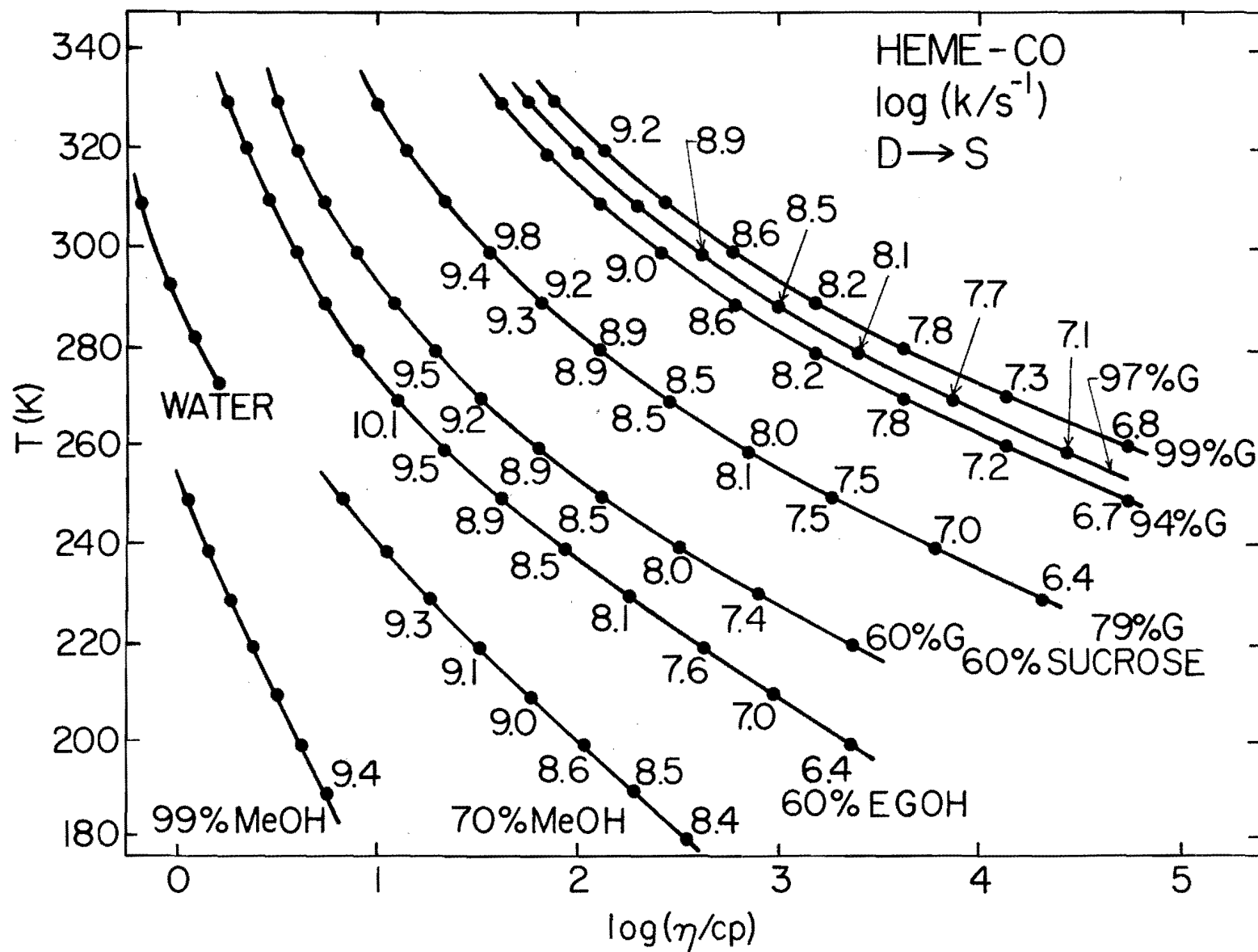
$$\lambda = \begin{cases} \lambda'[\text{Mb}] & \text{when } [\text{Mb}] \gg [\text{L}] \\ \lambda'[\text{L}] & \text{when } [\text{L}] \gg [\text{Mb}] \end{cases} \quad (1)$$

By measuring in both regions and determining [Mb] on a Cary 14 spectrophotometer, one can calculate  $\lambda'$  and [L]. Results were within 10% of the published values and [L] appears to level off (around 300 uM) at high glycerol percentages.

Figure 5

Region of temperature (T) and viscosity ( $\eta$  in cp=.01poise) where kinetics were measured. The solid lines are fixed solvent lines, which are mixtures of water with various cosolvents, percent by weight (G=glycerol, EGOH=ethylene glycol, MeOH=methanol). For example, 79% glycerol and 60% sucrose have a viscosity of about 800cp at 260K.

Values given are the log of the rate for CO to separate from protoheme after photodissociation. (see figure 16 for a diagram). Note that the values of the rate vary smoothly with viscosity. If other solvent properties were important, such as the dielectric coefficient, then abrupt changes should occur when the cosolvent is changed. These do not occur and it is assumed that the rate depends primarily on T and  $\eta$ .



#### D. Diffusivity measurements

The collision frequency of reactants in solution is proportional to the sum of their diffusivities. In order to test for a diffusion model, these diffusivities must be known. Usually one assumes Stokes law,  $D \propto T/\eta$ , which seems to be valid when changing the temperature for a single solvent (Abram and Mullen, 1972; Craig and Sutin, 1963). However, the reported diffusivities of molecules in glycerol are larger than expected. The measured diffusivities of O<sub>2</sub> versus glycerol percentage do not follow Stokes law, but are closer to a  $1/\sqrt{\eta}$  dependence (Jordan, Ackerman, and Berger 1956). We verified this fast diffusion by measuring the fluorescence of pyrene-butyric acid with and without oxygen quenching. Data for the fluorescence lifetime versus percent glycerol were available (Vaughan and Weber, 1970). Measuring the amount of steady state fluorescence versus oxygen pressure (up to 100 atm) determines the collision frequency,  $k_D[\text{O}_2]$ :

$$F_0/F = 1 + \tau k_D[\text{O}_2] \quad (2)$$

F and F<sub>0</sub> are the fluorescence with and without quenching and  $\tau$  is the lifetime of the fluorescence. If one knows  $\tau$  and [O<sub>2</sub>], then  $k_D$  and the diffusivity (see appendix A) can be determined. The results verified that the diffusivity is much larger than expected. Only lower limits were obtained due to the long equilibration times of glycerol with oxygen in the pressure cell.



### III. RESULTS

#### A. Kinetics of Mb-CO and Mb-O<sub>2</sub>

The recombination kinetics of CO to Mb versus temperature in 79% glycerol are shown in figure 6. Plotted on a log-log scale is the fraction of the Mb that have not recombined to a ligand versus time. At the highest temperatures the recombination appears as a single exponential process. As the temperature is lowered, additional processes become observable. A total of 4 processes are seen for Mb-CO, 3 for Mb-O<sub>2</sub>, and 2 for protoheme-CO. The faster processes are independent of ligand concentration, while the rate of the slowest process (IV) is proportional to the ligand concentration. At temperatures below 200K, only the fastest process I remains and the rebinding is not exponential (figure 7). A distribution of rates is required to simulate such kinetics. Process I is nearly independent of the solvent viscosity at low temperature. The results for Mb-O<sub>2</sub> in 90% glycerol are shown in figure 8. The kinetics at low temperature are similar to Mb-CO; however, at high temperature only 3 processes are seen.

#### B. Results in various solvents

The kinetics in various solvents at constant temperature are shown in figure 9. As the viscosity is increased, the

Figure 6

Recombination kinetics of CO to Mb in 79% glycerol w/w.  $N(t)$  is the fraction of Mb that have not rebound a ligand at time  $t$  after photodissociation. At 320K the kinetics consist of a single exponential process,  $N(t)=\exp(-kt)$ , with time constant  $1/k = 20\text{ms}$ . At lower temperatures, as many as four processes are observable. The rate of slowest process (IV) is proportional to the ligand concentration  $[\text{CO}]$ . The three faster processes are independent of  $[\text{CO}]$  for samples equilibrated with less than 10 atm of CO. The kinetics can be fit assuming the ligand encounters a series of four barriers when going from the solvent to the binding site.

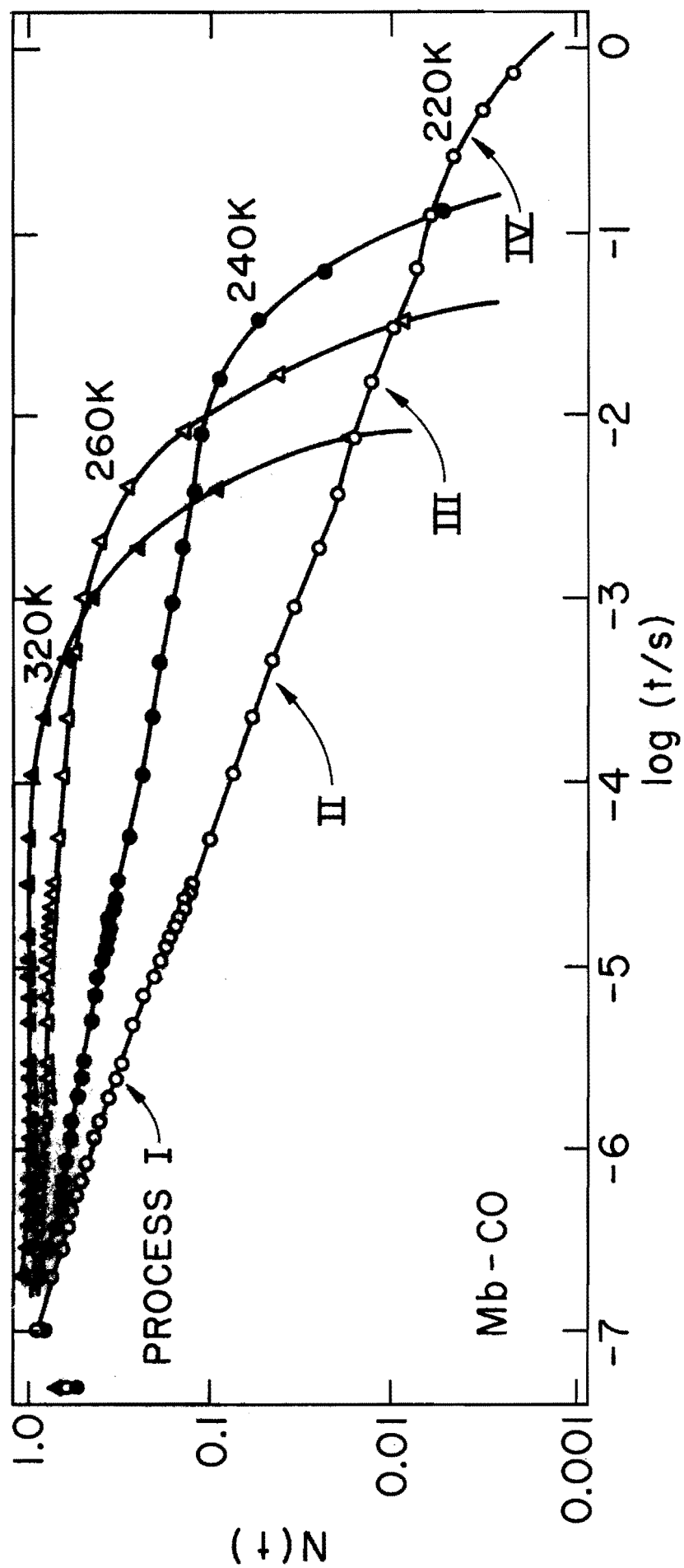


Figure 7

Recombination kinetics of CO to Mb at low temperature. Below 200K only process I is observed. The kinetics are not exponential but are close to power law:  $N(t) = (1 + t/t_0)^{-n}$ . These data can be fit with a distribution of rates, as if each Mb froze slightly differently and has its own rate. The results at low temperature are nearly independent of solvent. The data for Mb in a dried film of PVA, poly(vinyl alcohol), show the largest deviation.

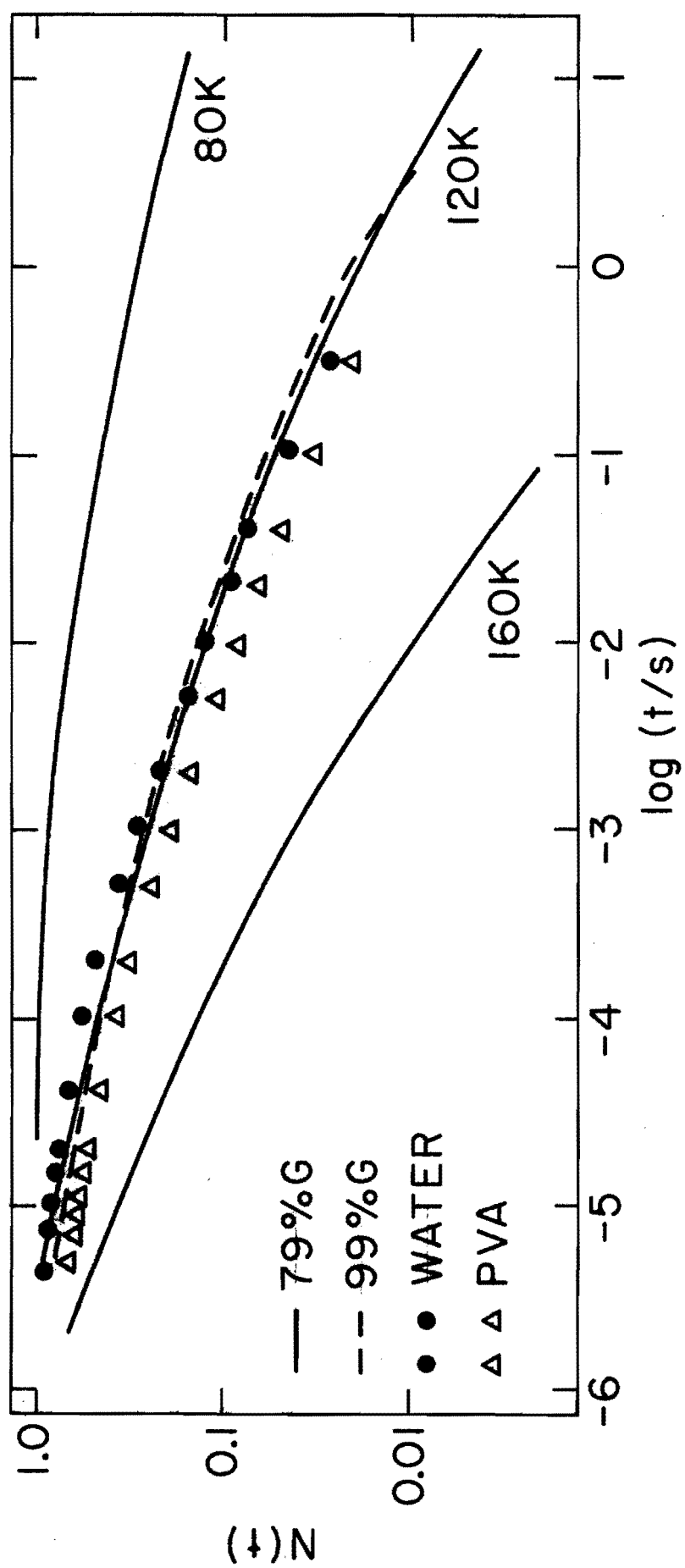


Figure 8

Recombination of O<sub>2</sub> to Mb in 90% glycerol.  $\Delta A$  is the change in absorbance of the sample at 436nm. Three processes are seen at 260K. As with Mb-CO, the kinetics below 200K are nonexponential. Process I appears to relax from the distribution of rates toward a single rate around 260K. The initial increase of the curve is simply the rise time of the electronics.

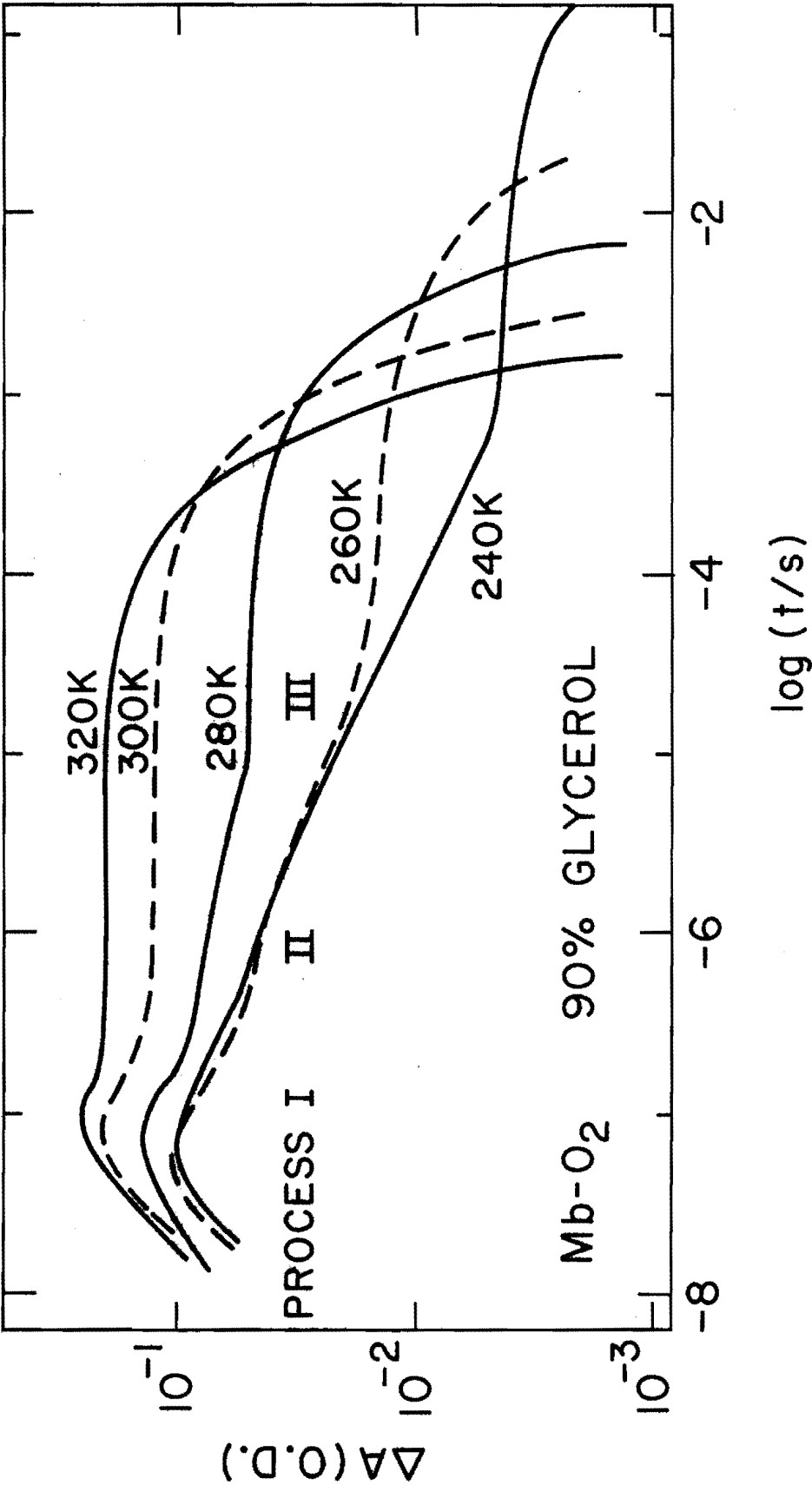


Figure 9

Kinetics in various solvents at fixed temperature for protoheme-CO, Mb-O<sub>2</sub>, and Mb-CO. Percentages refer to the cosolvent by weight (G = glycerol, EGOH = ethylene glycol, MeOH = methanol). As the viscosity increases, the rates decrease and fewer ligands rebind via the slower processes. All O<sub>2</sub> data are for samples equilibrated with air, except for 99% glycerol (one atmosphere of oxygen).



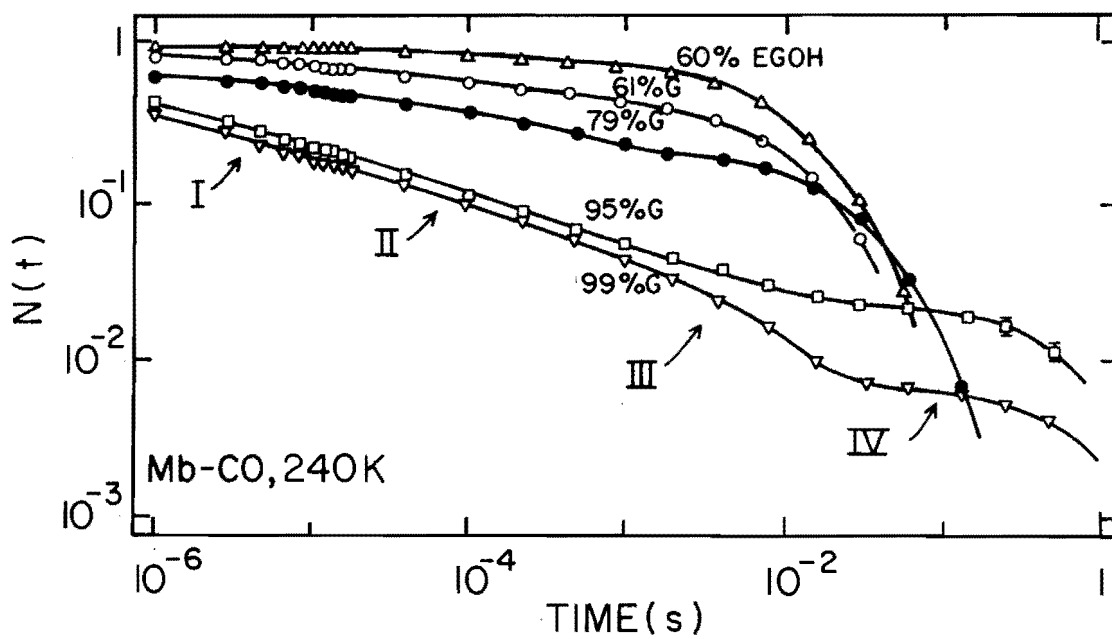
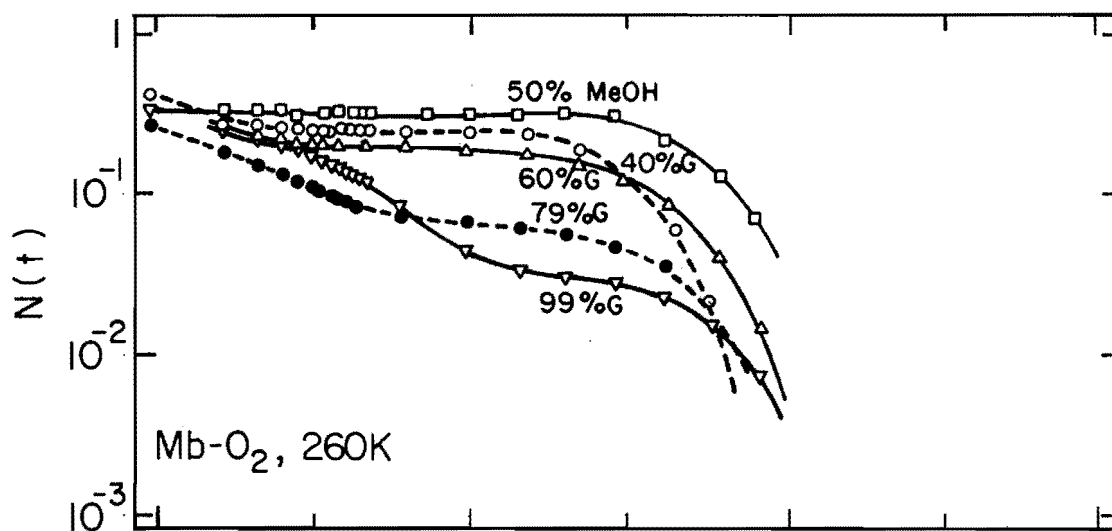
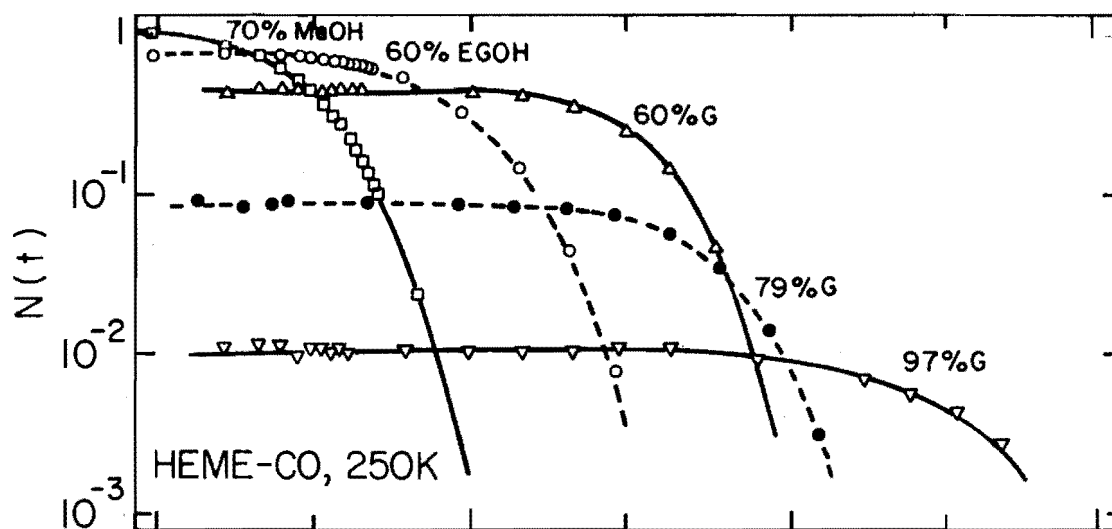
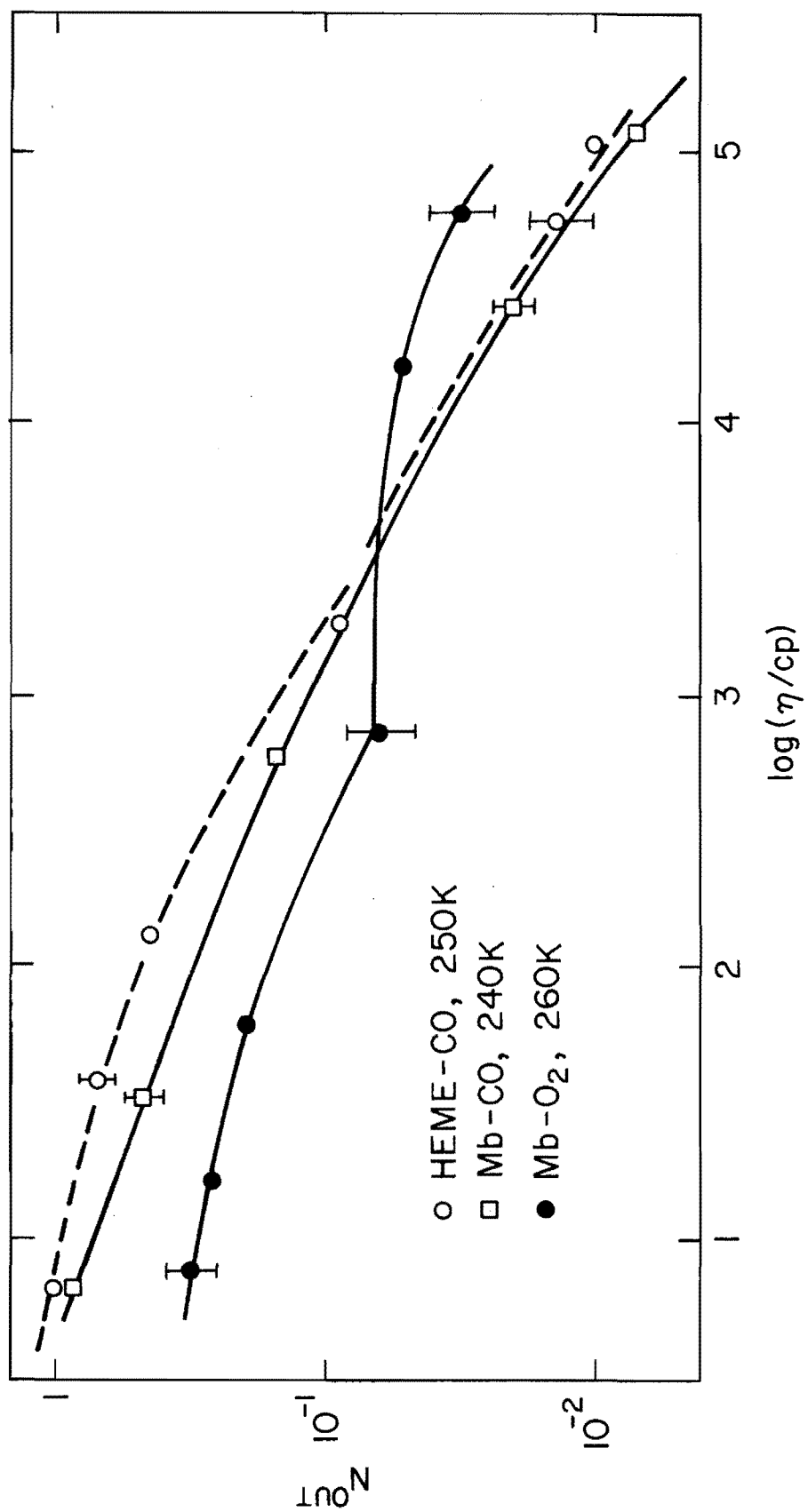


Figure 10

$N^{\text{out}}$  versus viscosity at fixed temperature.  $N^{\text{out}}$  is the fraction of photodissociated ligands that enter the solvent (the normalized amplitude of the slowest process). Fewer ligands are able to enter the solvent at high viscosity.



rates become slower and  $N^{\text{out}}$ , the fraction of photodissociated ligands which rebind via the slow process IV, decreases (figure 10).

In order to change the viscosity, the solvent must be changed and one should ask what other parameters have been altered. For example the dielectric constant and pH of the various mixtures will differ. The pH was varied from 6 to 10 in a given solvent without much effect on the data; therefore the variation of about one pH unit in the measurements is not important. Figure 5 shows the results for a single barrier for protoheme-CO. The values of the rate vary smoothly with viscosity. If the dielectric coefficient were important, discontinuities should appear when changing the cosolvent. Different solvents with the same viscosity (sucrose and glycerol) gave similar results, indicating the dominant effect is the viscosity.

### C. Errors in measurements

The best results obtained for the flash photolysis experiment approach a resolution of 1 part in 1000 for the transmitted light. At short times the photon noise of the monitoring system dominates (5% at 1  $\mu$ s). At long times the drift in the baseline is the main error (5% by 100s). These numbers represent the reproducibility while maintaining the same temperature. Data taken after returning to the same temperature agree with the original data within a few percent.

Sample to sample variation of the kinetics for Mb is less than 10%, except possibly for the rate of the concentration dependent process. Measurements at room temperature in closed cells with one atmosphere of CO or O<sub>2</sub> were used to determine the ligand concentration of all other samples. The kinetics of mixtures of protein and protoheme were also measured to obtain a better ratio of their rates under identical conditions.

There is an additional error due to the laser energy. When there is insufficient energy for complete photolysis the signal size will vary with the laser energy (5%). Measurements are made 3 times at each temperature to help average out this effect. When there is excess energy and some recombination occurs during the laser pulse, some ligands may be flashed off more than once. With the lus laser this problem was small for Mb-CO but does introduce error in the Mb-O<sub>2</sub> data. The multiple pumping makes the amplitudes of the slower processes larger. This pumping can be detected by varying the laser energy at a few temperatures or by comparing to a faster laser. The error is largest for the protoheme (almost a factor of 2 in some rate parameters), but the error can be reduced by measuring at a lower laser energy.

## IV. ANALYSIS

## A. Reaction rate theory

This section will describe the method of fitting the data and finding a model to explain the overall temperature and viscosity dependence. The thermodynamic formalism shall be introduced using a simple example and then the more complex kinetics will be considered. The relevant variables are:

$$\begin{array}{ll}
 V = \text{volume} & (\text{m}^3/\text{mole}) \\
 T = \text{temperature} & (\text{K}) \\
 P = \text{pressure} & (\text{kg}/\text{ms}^2) \\
 E = \text{energy} & (\text{kJ}/\text{mole}) \\
 H = \text{enthalpy} & (\text{kJ}/\text{mole}) \quad H = E + PV \\
 S = \text{entropy} & (\text{kJ}/\text{mole K}) \\
 G = \text{free energy} & (\text{kJ}/\text{mole}) \quad G = H - TS
 \end{array}$$

The simplest case would be a single process over a barrier of height  $E$ . The temperature dependence of a reaction is given by the Arrhenius form:

$$k = A e^{-E/RT} \quad \text{(s}^{-1}\text{)} \quad (3)$$

The energy term represents the fraction of reactants (constrained to a Boltzmann distribution) that would have enough kinetic energy to traverse the barrier. Typical barrier heights are 10-50 kJ/mole, where 100kJ/mole = 23.9kcal/mole = 1.04 eV/molecule. The pre-exponential represents the collision or attempt frequency of the reactants. Since most reactions are much slower,  $A$  was written as the product of the collision frequency and the probability of reacting after collision. This probability was

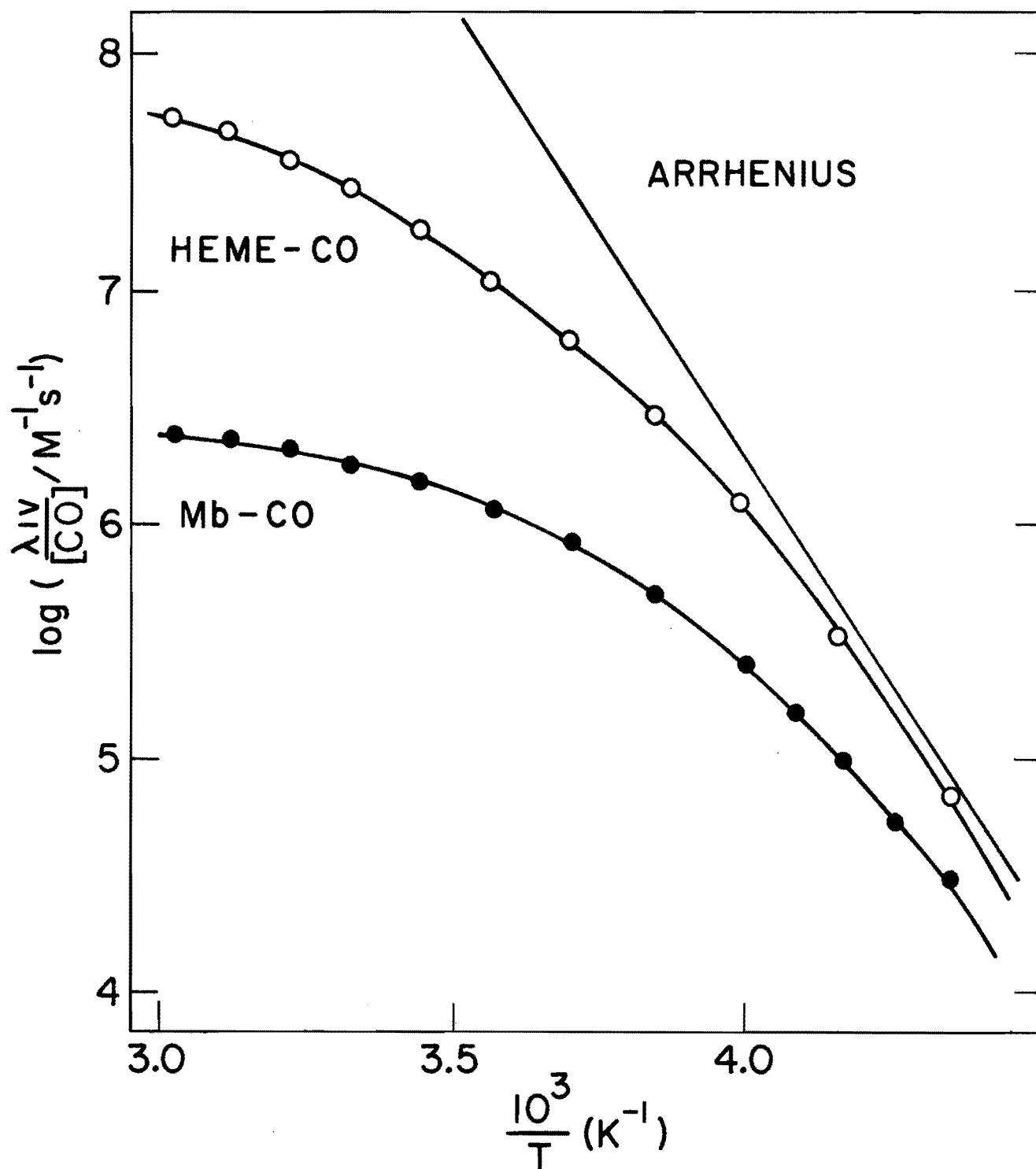


Figure 11

The rate of the slowest process  $\lambda_{IV}$ , corrected for the ligand concentration, versus  $1000/T$ . A straight line on such a plot is called Arrhenius behavior.

later interpreted as an entropy or steric hindrance term. The rate is now written in transition state theory (Glasstone, Laidler, and Eyring 1941):

$$k = v e^{-G/RT} = v e^{S/R} e^{-H/RT} \quad (s^{-1}) \quad (4)$$

where the frequency factor  $v = 10^{13}/s$ . For a bimolecular reaction,  $v$  is replaced by  $v'c$ , where  $v' = 10^{11}/Ms$  and  $c$  is the concentration of the rate limiting reactant ( $M = \text{moles per liter}$ ). The entropy term can be thought of as steric hindrance or the number of states. The rate would be much slower if the reactant had to move through some narrow passage even though the enthalpy barrier was the same. The usual analysis is to plot  $\log(k)$  versus  $1/T$ . A straight line on such a plot is called Arrhenius behavior, with the slope being the enthalpy and the  $(1/T)=0$  intercept is  $v \cdot \exp(S/R)$ . Kinetics showing this simple behavior could be fit with 2 parameters over the entire temperature range. Figure 11 shows a straight line along with the data for the slow process IV of Mb-CO and protoheme-CO.

#### B. Multiple process kinetics

We shall next consider a two process system, such as protoheme-CO. At a single temperature 4 parameters are required to fit both the rates and amplitudes. In general there are three states, each with its own spectra. In the systems being studied all unbound states are spectrally



identical so the sum of the amplitudes is a constant. Therefore 3 parameters are sufficient for a single temperature and 6 Arrhenius parameters are needed to fit the data over a temperature range.

Two simple reactions schemes are possible:



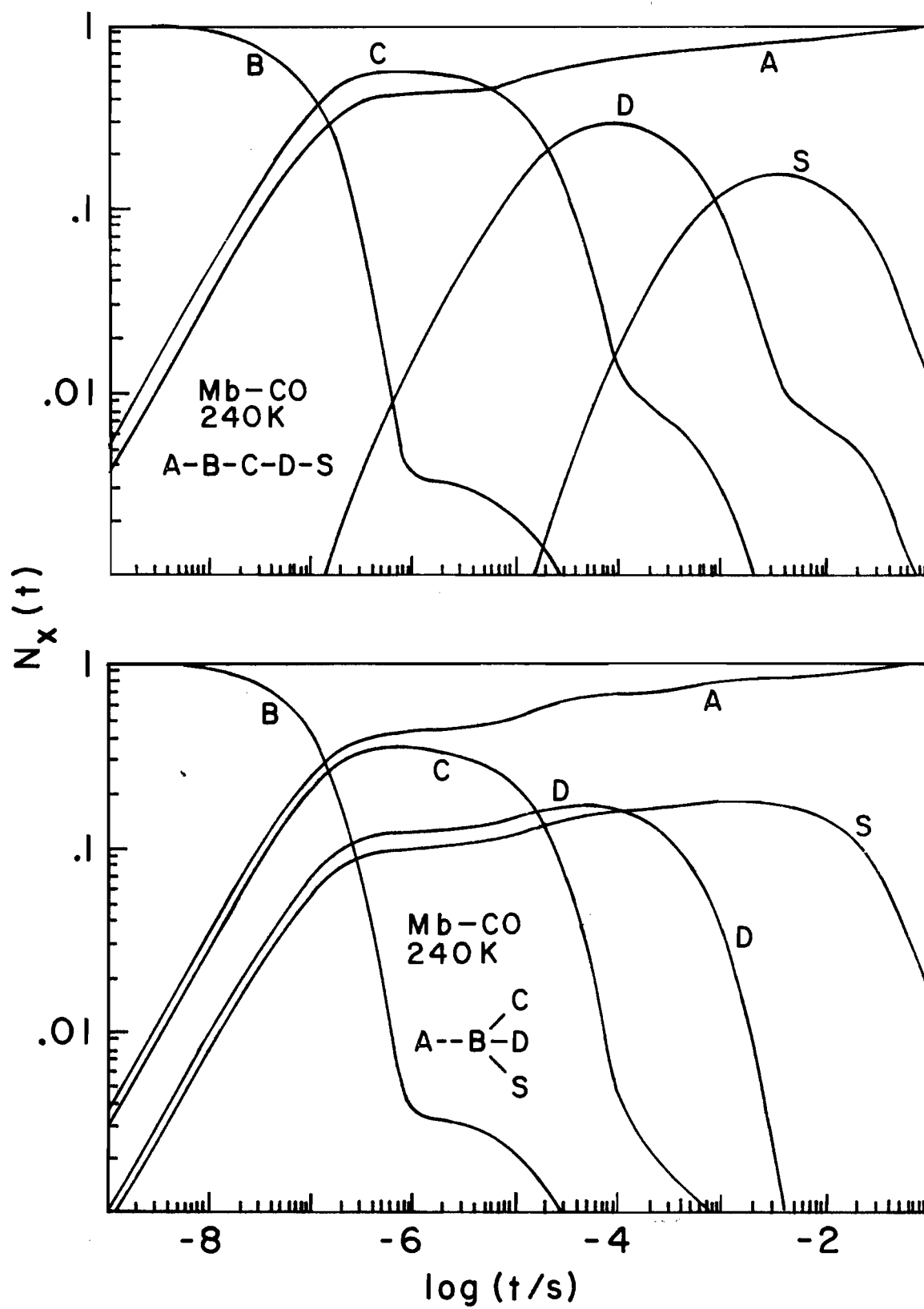
where A=binding site, S=solvent, and D is some intermediate state. It is assumed that the back reaction from the binding site A is negligible, as is the case for the heme proteins studied (Antonini and Brunori, 1971). The rate of the slower of the two processes for protoheme-CO is proportional to the ligand concentration and it is assumed that this process originates from the solvent S. The observed rates for the two processes are not Arrhenius. The branched model would require extra parameters to fit this behavior. The sequential model can fit the data with Arrhenius parameters, the observed rates being combinations of the rate parameters:

$$\lambda_I = \frac{k_{DA}}{k_{DA} + k_{DS}} \qquad \lambda_{IV} = \frac{\frac{k_{SD}}{k_{SD} + k_{DA}}}{\frac{k_{SD}}{k_{SD} + k_{DA}} + \frac{k_{DA}}{k_{DA} + k_{DS}}} \qquad (5)$$

The sequential model is preferred since it explains the curvature in the Arrhenius plot, figure 11. In fitting the protoheme data it is assumed that all the ligands are in well D immediately after the laser pulse. This fixes the total amplitude, and the amplitude of the slow process is determined

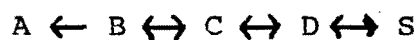
Figure 12

A computer simulation of the population of each well versus time for two models used to fit the kinetics of Mb-CO. Well A represents the binding site, S the solvent. It is assumed that the laser pulse takes all ligands from A to B. The experiment measures only the fraction in well A. In the branched model, a photodissociated ligand would make it out to the solvent in less time than in the sequential model. A probe of the outer wells is required to distinguish the many models that will fit the data.

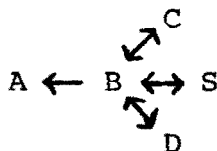


by the 3 parameters.

For more complicated systems, there are many possible models. Consider Mb-CO where 4 processes are observed. Fitting data without any model would require 8 parameters to fit four rates and four amplitudes. The processes do not show an Arrhenius behavior (figure 11) and  $8N$  parameters would be required to fit the data at  $N$  temperatures. Clearly a model with 16 Arrhenius parameters would be preferable, with the possibility of making some physical assumptions to further reduce the number. First note that four processes implies the existence of five states with 20 possible interconnections. One such model would be a series of four barriers:



where A represents the binding site within the protein and S represents the solvent. Since the step AB is negligible, this model requires 7 parameters (14 for all temperatures) to fit the kinetics. Other models can fit the data at any single temperature, however some do not allow the large reduction in parameters which is possible when the parameters are Arrhenius. For example, models which connect S directly to A will need several parameters to fit the curvature in process IV (figure 11). There are other Arrhenius models, such as:



This branched model represents the other extreme from the

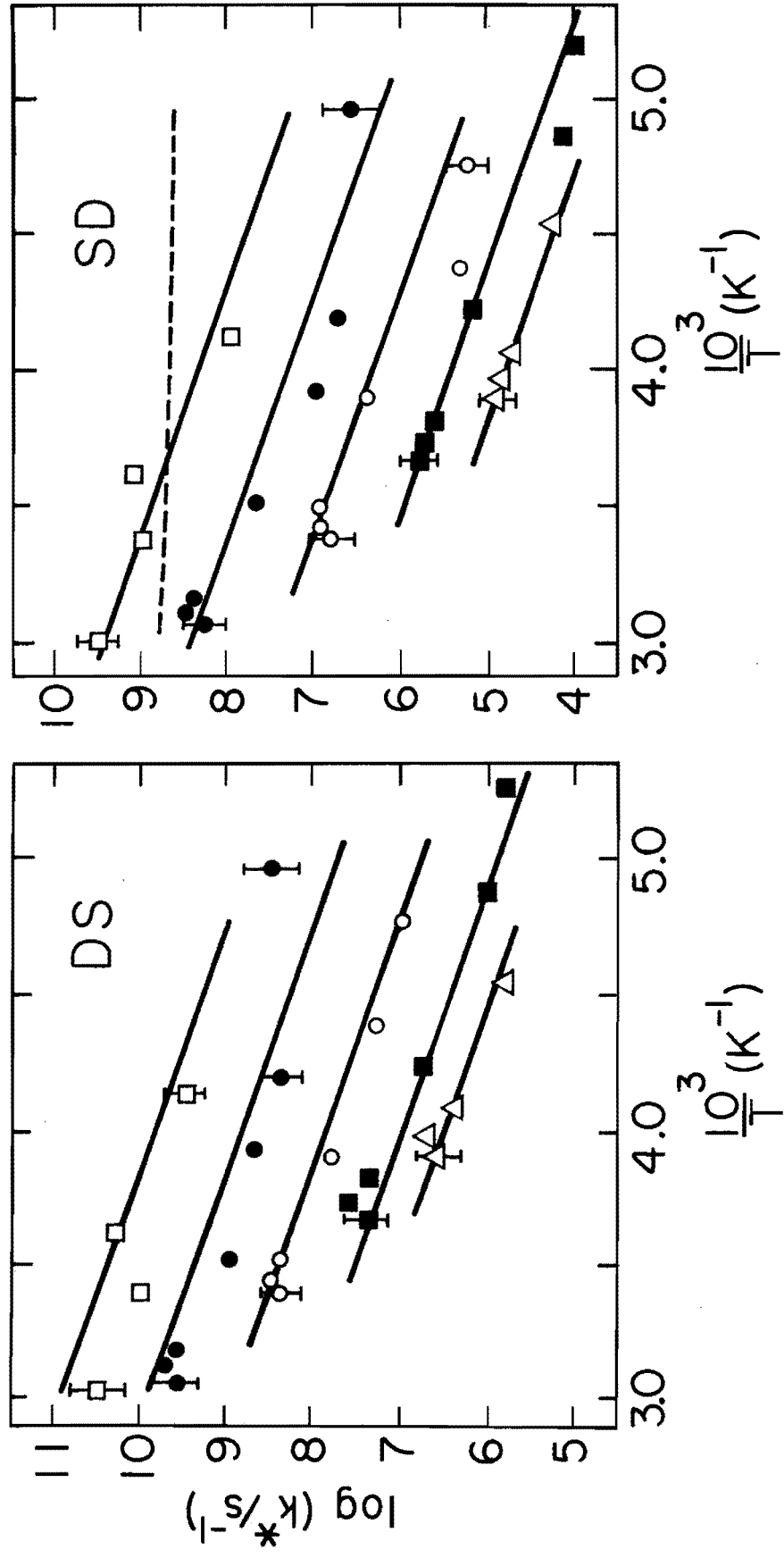
sequential one. Both require 14 parameters to fit the data. They differ in the time dependence of the population of all states except A (figure 12). Unfortunately, the flash photolysis experiment only determines if the ligand is in A or not - no information is given about the other wells since they all have the same absorption coefficient in the region monitored. Therefore, several models will fit the data, which is the population of well A.

There is one nice feature the sequential model has - the enthalpy is nearly the same when crossing a given barrier in either direction ( $H_{ij} = H_{ji}$ ). This reduces the total number of parameters for an entire temperature region to 11. The results for fitting the data versus temperature for the solvent 79% glycerol are shown in table I.

Next the viscosity dependence of the kinetics shall be considered. As the temperature is lowered the rates decrease for two reasons: the energy barrier and the viscosity dependence. The previous Arrhenius analysis should be applied only when all other relevant parameters have been held constant. Data taken in a single solvent are not sufficient to extract information on both the barriers and the viscosity dependence. The fact that Arrhenius parameters were obtained is not a coincidence. Over the range of temperatures considered the viscosity also has an Arrhenius temperature dependence:  $\eta \propto \exp(\Delta/RT)$ . If the rate varies as  $\exp(-H/RT)$  at

Figure 13

Arrhenius plots of the rates DS (from well D to S) and SD for protoheme-CO (see figure 16) at five viscosities ( $\log(\eta/\text{cp}) = 1, 2, 3, 4, 5$ ;  $\square, \bullet, \circ, \blacksquare, \triangle$ ). The solid lines are results of fitting all the data to the form  $k(T, \eta) = (A_0 + A/\eta^\kappa) \exp(-H/RT)$ . Thus a single barrier is fit with four parameters,  $H$  being the slope and  $\kappa$  adjusting the spacing of the isoviscosity lines. The dotted line is a simple diffusion model, assuming the rate varies as  $T/\eta$ . Units for the process SD are  $\text{M}^{-1}\text{s}^{-1}$ .



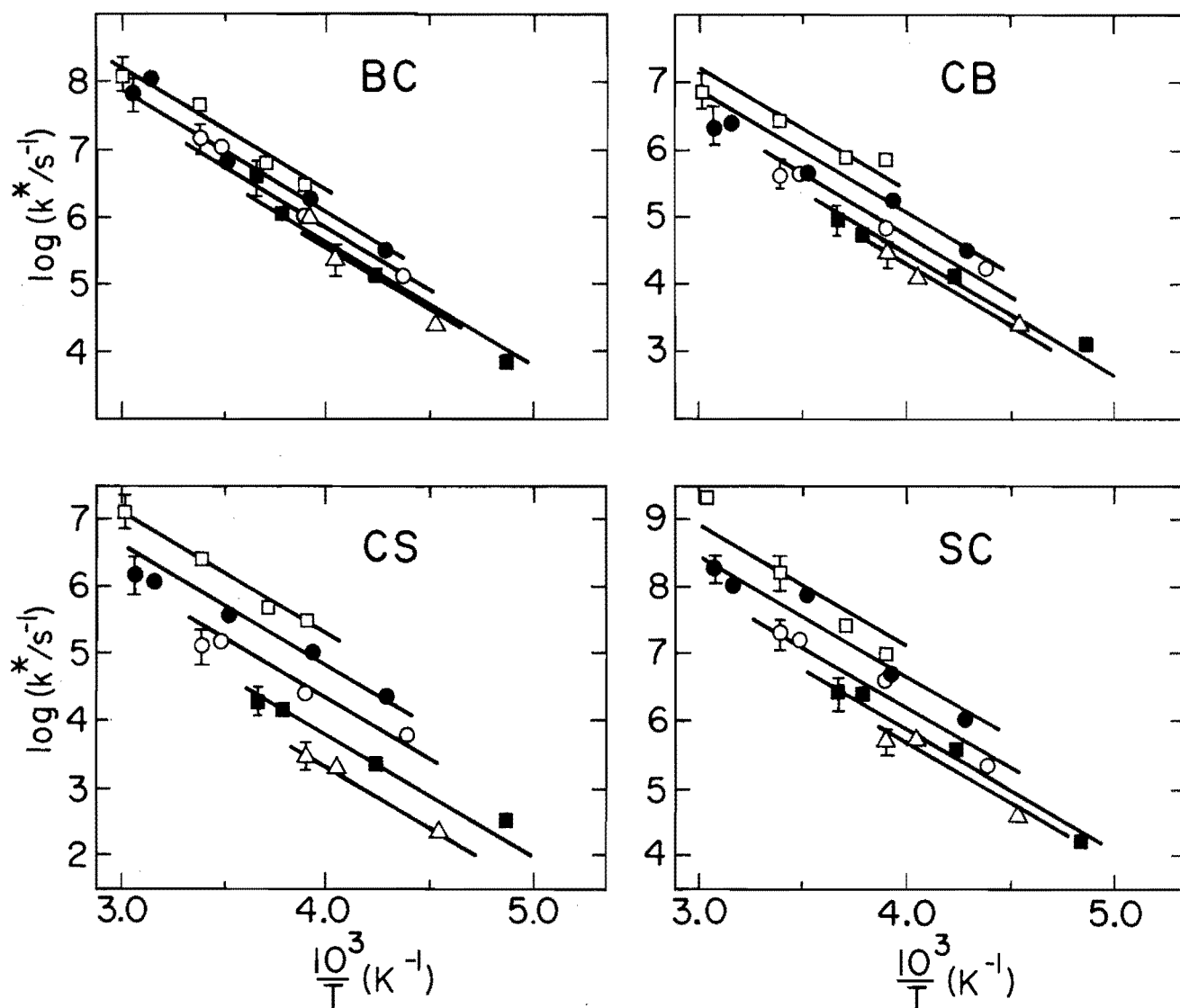


Figure 14

Arrhenius plots of the rates for Mb-O2 at  $\log(\eta/cp)=1, 2, 3, 4, 5$ .

Symbols as in figure 13. Units for the rate SC are  $M^{-1}s^{-1}$ .



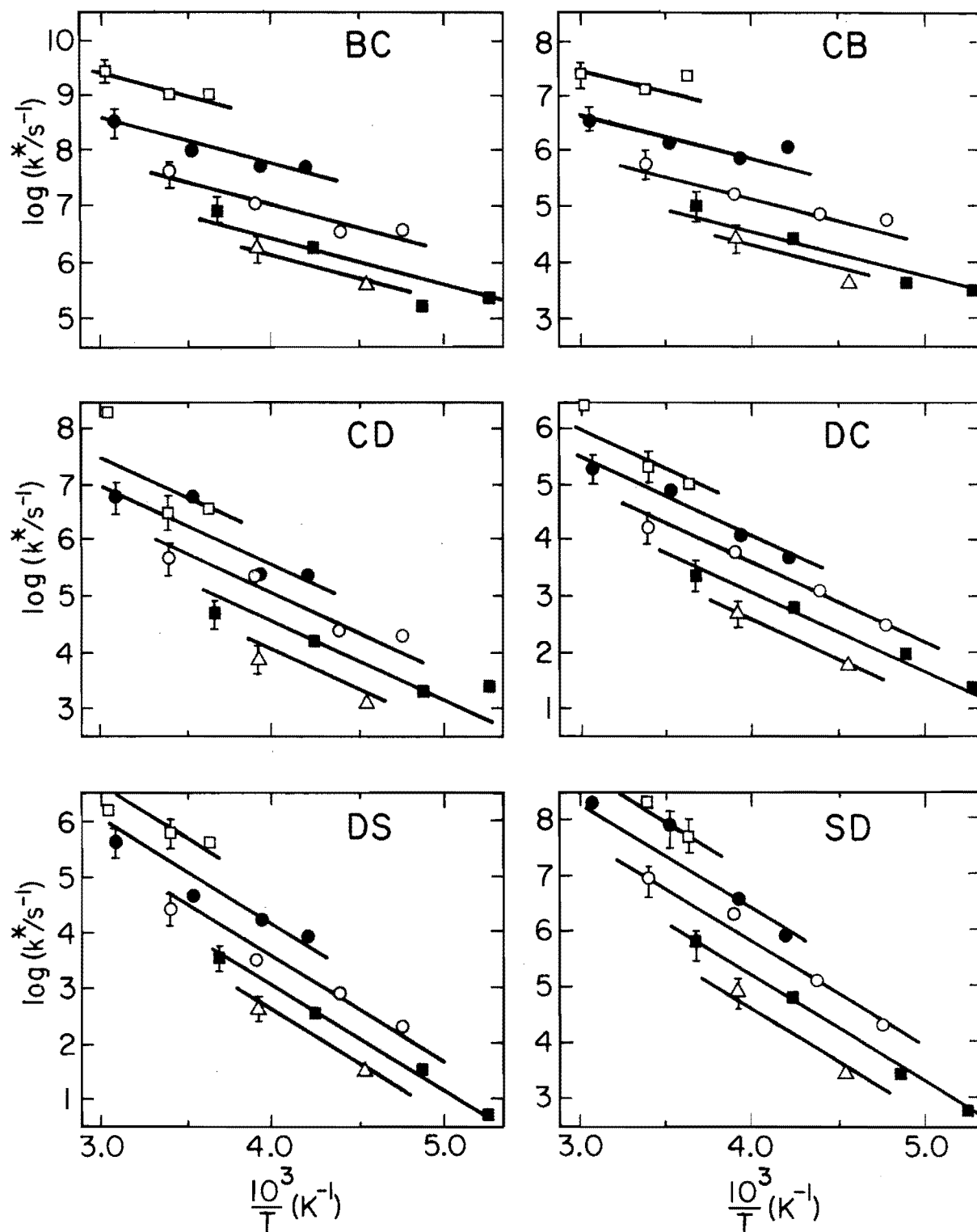


Figure 15

Arrhenius plots of the rates for Mb-CO at  $\log(\eta/cp)=1, 2, 3, 4, 5$ .

Symbols as in figure 13. Units for the rate SD are  $M^{-1} s^{-1}$ .

constant viscosity and varies as some power of the viscosity ( $k \propto 1/\eta^K$ ), then the temperature dependence of the rate in a single solvent will be  $\exp[-(H+\kappa\Delta)/RT]$ . The two exponential effects will simply add to some effective enthalpy for the protein-solvent system.

The Arrhenius plots for all the barriers at five viscosities are shown in figures 13,14 and 15. The plots for heme show an Arrhenius behavior with a  $1/\eta$  dependence until the rates tend toward some limit at the highest viscosity. Process I is nearly independent of viscosity and is not shown. The results for the proteins are similar, but the spacing of the constant viscosity curves is less. This can be fit by using a power of viscosity less than one. The solid lines are fits to:

$$k(T, \eta) = (A_0 + A/\eta^K) e^{-H/RT} \quad (6)$$

H is now the viscosity independent enthalpy barrier and  $A_0$  is simply a saturation term. The values are tabulated in table II. After the initial fitting, it became apparent that the H and  $\kappa$  were nearly the same for traversing a barrier in either direction.

In summary we used the following method to determine both the temperature and viscosity dependence of the kinetics:

1. Data were taken from 200-350K every 10K in many solvents.
2. A model was chosen (sequential) and the kinetics were fit with the rate coefficients at each temperature where all processes can be seen.

3. The rates for all solvents were interpolated along isoviscosity lines (figure 3) at  $\log(\eta/c_p) = 1, 2, 3, 4, 5$ .
4. Arrhenius plots were made for each barrier for all 5 viscosities (figures 13, 14, 15)
5. The overall plots were then fit to the form of eq. 6.

The main features are:

- (a) the rates vary as  $1/\eta^{\kappa}$  with  $0 < \kappa < 1$ .
- (b) the rates tend toward a limit at high viscosity
- (c) the enthalpy and viscosity exponent are independent of the direction of crossing the barrier:  $H_{ij} = H_{ji}$  and  $\kappa_{ij} = \kappa_{ji}$

Features (a) and (b) are independent of the model chosen.

Feature (c) is true for the sequential model.

#### C. Error analysis

The measurements are accurate enough to determine rates for a single process to within 5%. However, the multi-phase kinetics lead to errors due to the coupling of the fitting parameters. Poor choices of the parameters for the faster processes will propagate to the parameters involved in all slower processes. This is clear when looking at an approximate form for the rate of process IV for Mb-CO:

$$\lambda_{IV} = k_{SD} \left( \frac{k_{DC}}{k_{DS} + k_{DC}} \right) \left( \frac{k_{CB}}{k_{CD} + k_{CB}} \right) \left( \frac{k_{BA}}{k_{BC} + k_{BA}} \right) \quad (7)$$

Based on how much the individual parameters can be varied and still fit the data, errors in the  $k$ 's may be as large as a factor of two. Error propagation via coupling of parameters

can be worse if one assumes an Arrhenius form and fits with H and S. It is better to fit with k's and then look for Arrhenius behavior or some other correlation of the rates. Using H and S couples the temperatures as well as the different processes. Although H and S are poorly determined, the difference between H and S for a given barrier is better determined. In order of increasing error: observed rates (data), rate parameters k or  $G=H-TS$ , the difference between H's or S's, and finally the precise value of H or S.

Although errors as large as a factor of two may occur in the k's, the effect of temperature or viscosity on the rates is two orders of magnitude larger. Thus the overall trends can be well described.

Table I.

Activation enthalpies (H) and entropies(S)

	Sequential model				Branched model		
	Iso-solvent (79% glycerol)		Iso-viscosity (1 poise)		Iso-solvent (79% glycerol)		
	H	S/R	H	S/R	H	S/R	
protoheme-CO							
DA	1.	-9.2	1.	-9.2			
DS	60.	16.5	20.	-0.2			
SD	74.	24.	22.	2.3			
Mb-O2							
BA	8.8	-10.4	8.8	-10.4	8.8	-10.4	
BC	46.	5.4	40.	3.3	34.1	-0.7	
CB	42.	0.8	30.	-4.0	50.2	5.0	
CS	59.	7.8	30.	-4.4	57.4	9.6	(BS)
SC	61.	18.6	40.	9.0	54.2	15.3	(SB)
Mb-CO							
BA	10.	-9.9	10.	-9.9	10.	-9.9	
BC	54.	11.4	16.	-4.3	32.3	-0.2	
CB	45.	3.8	15.	-9.2	30.	-4.6	
CD	70.	16.	25.	-4.8	41.1	2.9	(BD)
DC	56.	5.7	28.	-7.1	39.	-4.2	(DB)
DS	58.	5.3	28.	-6.9	47.	5.6	(BS)
SD	80.	26.2	40.	8.7	39.	4.8	(SB)

Units for H and TS in kJ/mole

 $R = 8.31 \text{ J/mole K}$  (gas constant) $k_B = 1.38 \cdot 10^{-23} \text{ J/K}$  (Boltzmann's constant) $N = 6.02 \cdot 10^{23} / \text{mole}$  (Avogadro's number),  $R = k_B N$

Table II.

Parameters for modified Kramers equation

$$k(T, \eta) = (A_0 + A/\eta^\kappa) e^{-H/RT}$$

Best Fit					Coupled H and $\kappa$			
	logA <sub>0</sub>	logA	$\kappa$	H	logA <sub>0</sub>	logA	$\kappa$	H
protoheme-CO								
DS	10.7	14.9	1.0	20	10.8	15.2	1.0	21
SD	9.2	14.	1.0	22	9.0	13.7		
Mb-O <sub>2</sub>								
BC	13.8	14.8	.3	40	12.8	14.1	.4	35
CB	10.5	12.2	.5	30	11.4	13.1		
CS	-	12.1	.5	30	<10.5	13.1	.5	35
SC	13.8	15.7	.4	40	12.9	14.9		
Mb-CO								
BC	9.4	12.7	.8	16	9.1	12.5	.8	15
CB	7.4	10.6	.8	15	7.4	10.6		
CD	-	12.1	.6	25	<8.5	12.2	.5	27
DC	-	10.9	.5	28	<8.0	10.7		
DS	7.8	11.4	.7	28	9.7	12.8	.6	36
SD	-	16.0	.6	40	<12.0	15.1		

Units: H in kJ/mole, A<sub>0</sub> in s<sup>-1</sup>,  $\eta$  in cp, A in s<sup>-1</sup>(cp) <sup>$\kappa$</sup> ,except for SD, SC, or SB: A<sub>0</sub> in M<sup>-1</sup>s<sup>-1</sup>, A in M<sup>-1</sup>s<sup>-1</sup>(cp) <sup>$\kappa$</sup> 

Viscosity: 1 poise = 100 cp = 1 g/cm s

For certain rate coefficients, A<sub>0</sub> was not needed. Only an upper limit is given.

## V. Interpretation

### A. Fluctuating protein model

The model used to fit the data consists of a series of barriers. The barriers at 260K for two viscosities are shown in figure 16. The laser pulse takes the ligands from the binding site (well A) to well B. The ligands may then rebind or wander farther away to well C. The rates for going in either direction will determine what fraction migrate outward and make it to wells C,D, and S, the solvent. The potential surface shows that the equilibrium properties are not effected by the viscosity. Only the time to traverse the barrier changes.

The dependence of the rate versus viscosity at constant temperature (260K) is shown in figure 17. The plots show the logarithmic dependence and also that the rate tends toward some limit at high viscosity. The values for Mb-CO extrapolate nicely to the results obtained for samples in a thin film of PVA, which could be considered as a very high viscosity solvent.

Consider a model for Mb where the protein can fluctuate between two states (figure 18): when closed the ligand is trapped and when open the ligand is free to pass. The actual barrier is then one of the protein motion, although the presence of the ligand probably influences the motion. This model explains why  $H$  and  $\kappa$  are the same for crossing the

Figure 16

The free energy  $G^*$  (\* indicates all solvents considered together) versus reaction coordinate for the sequential barrier model. Viscosity changes the rate for crossing a barrier, but does not change the equilibrium properties.  $G$  for well B (D for protoheme-CO) is defined as zero. Well A would be at -55 kJ/mole for Mb-CO, -30 kJ/mole for Mb-O<sub>2</sub>.



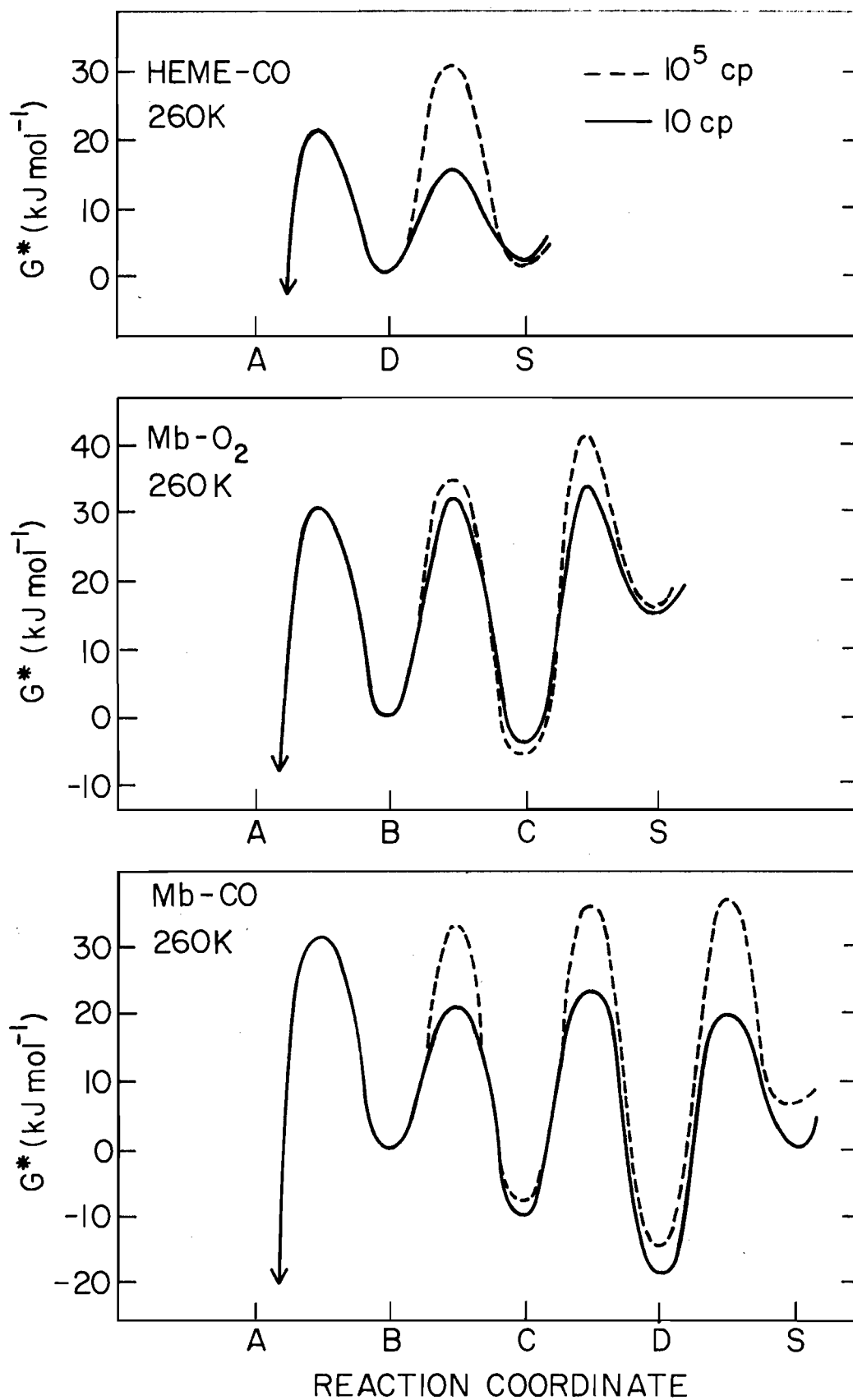


Figure 17

The rates for the various barriers versus viscosity at fixed temperature. The dotted lines in the heme-CO plot are slope -1. The values for Mb-CO extrapolate nicely to the results obtained for samples in dried films of PVA, poly(vinyl alcohol), which can be thought of as a very high viscosity solvent. Units for the transitions SD and SC are  $M^{-1}s^{-1}$ .

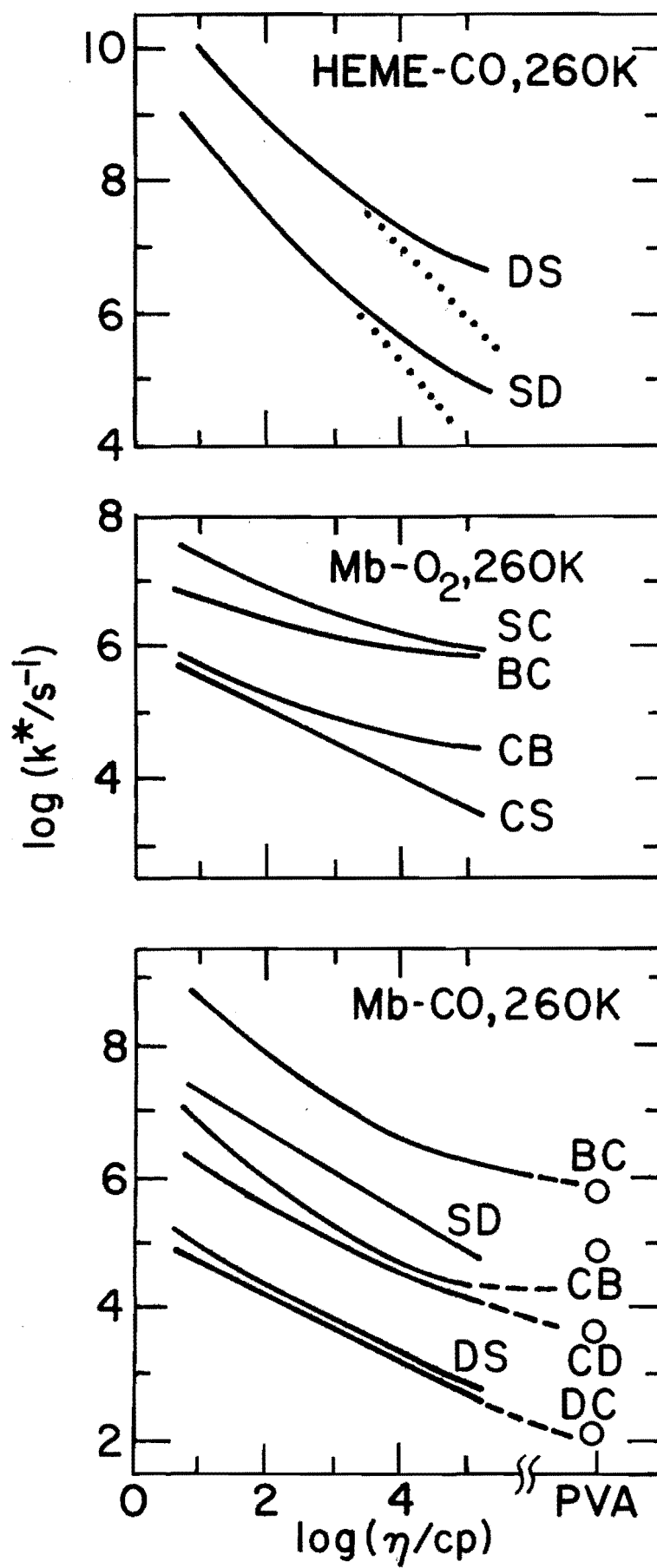
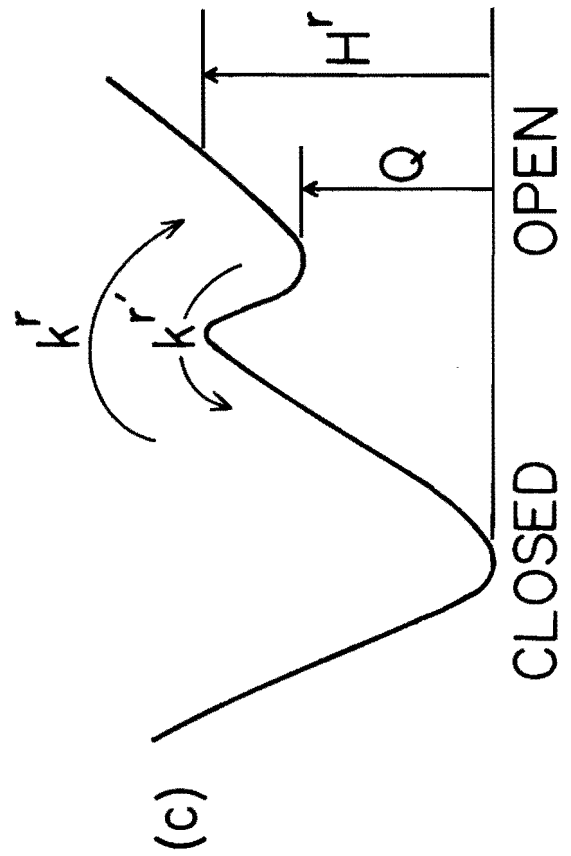
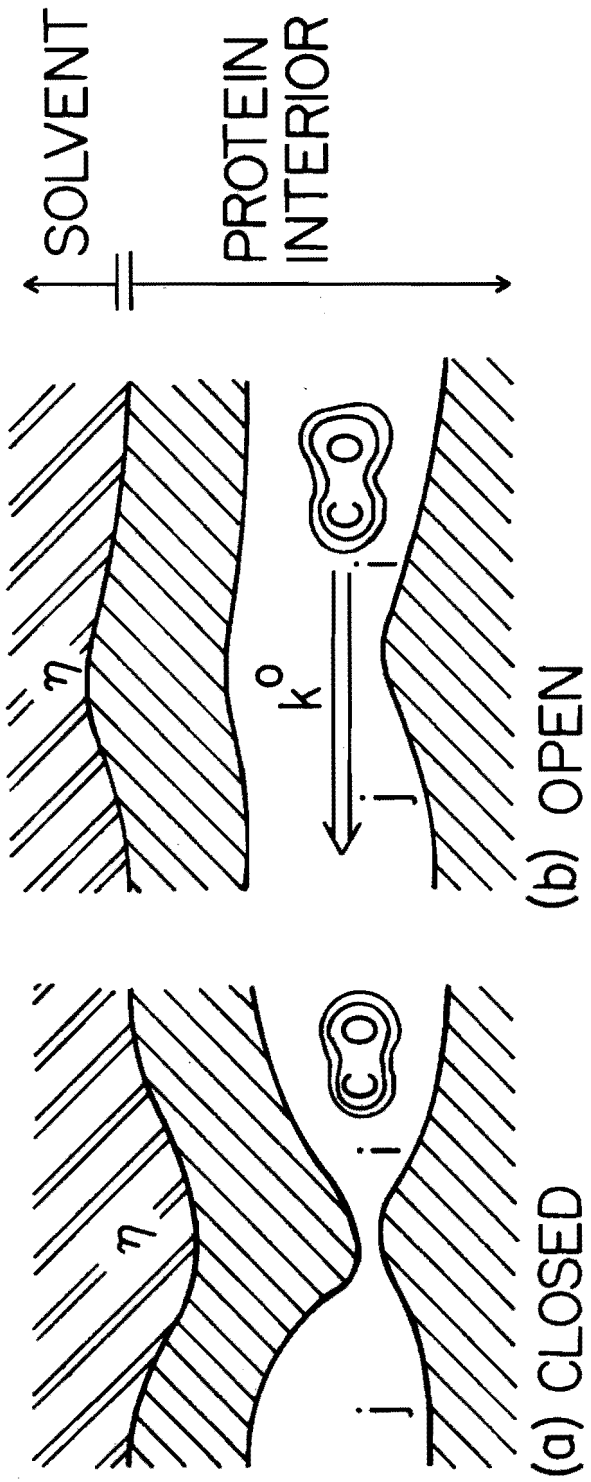


Figure 18

A model of how protein motion governs the reaction rates. The protein can exist in two states. In the closed state, the ligand is trapped. When open the ligand is free to pass. Thus the measured rates are for the protein fluctuations which are influenced by the solvent properties.



barrier in either direction. The value of  $\kappa$  would depend on how the protein structure shields the external viscosity.

## B. Internal viscosity

On a large scale viscosity represents the drag force on an object or on the fluid itself. At the microscopic level, there are collisions between molecules. The net effect of these collisions leads to the observable drag forces, however a given particle or oscillator will experience a wider spectrum of motions.

Consider a damped harmonic oscillator of natural frequency  $\omega = \sqrt{k/m}$ , which is described by the Langevin eq.:

$$m\ddot{x} = -kx - f\dot{x} + G(t) \quad (8)$$

Here the damping force is written explicitly as  $f\dot{x}$ , where the Stoke's friction constant  $f = 6\pi\eta r$ . The random force  $G(t)$  guarantees that the system is kept in thermal equilibrium:  $(1/2)k_B T$  average energy for each degree of freedom. Such a system rapidly goes from underdamped to overdamped (within a factor of 2-3 in viscosity). This transition occurs when  $f=2\omega$  or  $\eta = (m/r)(\omega/3\pi)$ . For the systems being considered,  $m/r=10^{14}$  g/cm and  $\omega=10^{11}$  to  $10^{14}$ /s; the critical viscosity would then be in the range .01 to 1cp. This result would imply that the protein in its natural environment is in the overdamped region; and even in water (1cp) the kinetics should be sensitive to the solvent viscosity.

If an oscillator in an internal region of viscosity  $\eta_i$  is coupled to an external oscillator in viscosity  $\eta$ , then two relaxation modes are present. The faster rate decreases as  $1/\eta$  for  $\eta < \eta_i$  and becomes constant for  $\eta > \eta_i$ . The slower mode is constant until  $\eta > \eta_i$  and then dies out as  $1/\eta$ . Thus coupled oscillators can explain the saturation of the experimental rates; however, a distribution of internal viscosities is needed to simulate the observed  $1/\eta^k$  dependence. From figure 17 the internal viscosity is estimated to be about 100 poise.

Using equation 8 assumes a certain frictional constant. The motion of ligand may be better described by a generalized Langevin equation (Kirkwood, 1946):

$$m\ddot{x} = K(x) + F(t) \quad (9)$$

$K(x)$  is the external force and  $F(t)$  is the intermolecular force. From this equation a fluctuation dissipation theorem can be derived (Kubo, 1966; Kirkwood, 1946; Chandrasekar, 1943). The friction coefficient is now frequency dependent, the drag force being the time integral of the correlation function of the random force (at the low frequency limit):

$$f(\omega) = \frac{1}{6k_B T} \int_{-\infty}^{\infty} \langle F(0)F(s) \rangle e^{-i\omega t} ds \quad (10)$$

The random force for the ligand is provided by the fluctuating protein which is influenced by the external environment. We can now ask what form the correlation function of the random force must have. In order to obtain the usual external

viscous force ( $f$ ), the function must have the form  $\exp(-t/t_c)$  with the correlation time  $t_c \propto 1/f$ . Usually  $t_c$  is taken to be very small and one can derive (Reif, 1965) the return to equilibrium of the velocity:  $v(t) = v(0)\exp(-t/m)$ . Thus the viscosity will determine the relaxation time of the system:  $m/(6\pi\eta r) = 10^{-16}$  s when  $m/r = 10^{-14}$  g/cm and  $\eta = 5$  poise.

To obtain the observed form  $\eta_i = \eta^k$ , a possible solution is  $(t/t')^{k-1} \exp(-t/t_c)$ , where  $t'$  is a characteristic time and there may be a distribution of such times describing how the system relaxes. For the observed rates, there must be some small  $t'$  indicating that there are some rapidly damped modes. The details of the microscopic forces are required to draw more specific conclusions. From the general description above, one can describe myoglobin as behaving like a collection of non-identical oscillators with a damping coefficient corresponding to an internal viscosity around 100 poise.



## Appendix A: Diffusion

When the reactants are originally separated, as for process IV, they must first collide before reacting. When the collision time is slow compared to the subsequent crossing of any barriers, the reaction is said to be diffusion controlled. The measured rate is then simply the collision frequency which the solvent would control. Since the current experiments involve high viscosity it is important to first decide whether the rates are barrier or diffusion controlled.

The collision frequency between reactants is the maximum rate at which the reaction can proceed. Smoluchowsky was the first to derive the steady state collision frequency for reactants with diffusivities  $D_X, D_Y$  ( $\text{cm}^2/\text{s}$ ) and interaction distance  $r$  ( $\text{cm}$ ):

$$k_D = .004 \pi N (D_X + D_Y) r \quad (\text{M}^{-1} \text{s}^{-1}) \quad (11)$$

When Stokes law applies  $D_X = k_B T / 6 \pi \eta r_X$ , where  $r_X$  is the radius of the diffusing particle.  $N$  is Avogadro's number. As mentioned in section II.D., the diffusivity of  $\text{O}_2$  versus glycerol percentage does not obey Stokes law. We will therefore use eq.11 with the measured diffusivities of the ligand (the diffusivity of the protein being negligible). We will use the full radii of the reactants and introduce a multiplicative constant  $s$  to represent any steric factors:

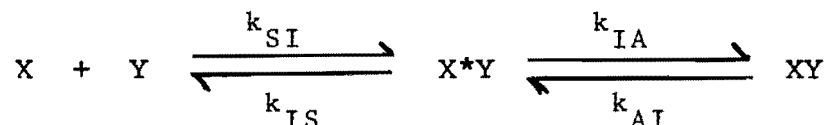
$$k_D = s (7.57 \cdot 10^{21}) D_L^r \quad (M^{-1} s^{-1}) \quad (12)$$

Typical values for O<sub>2</sub> diffusion in water at 298K are:

$$D = 2 \cdot 10^{-5} \text{ cm}^2/\text{s}, \quad k_D = 10^{10} \text{ (M}^{-1} \text{s}^{-1}\text{)}, \text{ for } s=1, r=6A.$$

If the binding rate were simply the collision frequency (full radii,  $s=1$ ), there would be no question that the reaction is diffusion controlled. However, the slow concentration dependent process being considered here requires  $s < .05$ . Usually a viscosity dependence is taken as evidence of diffusion, but the other reactions seen in Mb also show a viscosity dependence. We therefore need a better definition of diffusion controlled kinetics and some restrictions imposed on  $s$ .

Eigen has described the diffusional encounter followed by barriers as (Eigen, 1974):



where the subscripts represent the solvent(S), the binding site (A) and the interface region (I). The criteria for diffusion control is  $k_{IA} \gg k_{IS}$ . This guarantees that every

collision results in binding. In a flash photolysis experiment the ligand is faced with this same choice as it attempts to leave the protein. Therefore, in a diffusion controlled region, few ligands should make it out to the

solvent. At best one can test for consistency with a diffusion model when  $s \ll 1$ . For the analysis we will use eq (12) with:

- (1) the measured values of  $D_{O_2}$  at 298K and assume  $D_{CO} = D_{O_2}$ .
- (2) the assumption that  $D \propto T/\eta$  for a given solvent.
- (3) the radii term is 6A for protoheme and 15A for Mb.
- (4) the assumption that  $s$  is independent of temperature and solvent.

One can then compare the measured and calculated rates to see if the kinetics are consistent with a diffusion model with fixed  $s$ . The criteria for diffusion control will be :

- (a) the rates must scale with the measured diffusivities.
- (b) the fraction of the ligands entering the solvent must be small.

The second order rates for the slowest process,  $\lambda_{IV} / [L]$  ( $M^{-1} s^{-1}$ ), are shown in figure 19. A comparison to diffusion control is made by adjusting  $s$  so that the rates agree at the low temperatures for 99% glycerol(G). An  $s \approx 0.01$  is needed if the rates are to be considered diffusion limited (small interaction distance or steric hindrance). The rates are then consistent with the 2 criteria at the lower temperatures for solvents with more than 79% glycerol, except for Mb-CO.

Figure 20 shows the values of  $N^{out}$ , the fraction of dissociated ligands which leave the protein and rebind via process IV. The results are consistent with the requirement that  $N^{out}$  is small in the diffusion limited region.

Figure 19

The rate of the slowest process (IV) versus  $1000/T$ . The dotted lines are the calculated diffusion rate (eq. 12) using the measured diffusivities. The constant  $s$  was adjusted so the rates would agree at the low temperatures of the 99% glycerol solvent:  $s=.048$  for protoheme,  $.067$  for Mb-O<sub>2</sub>, and  $.027$  for Mb-CO. Percentages are glycerol by weight. The low temperatures of the high viscosity solvents are then in agreement with the diffusion rate, except for Mb-CO.

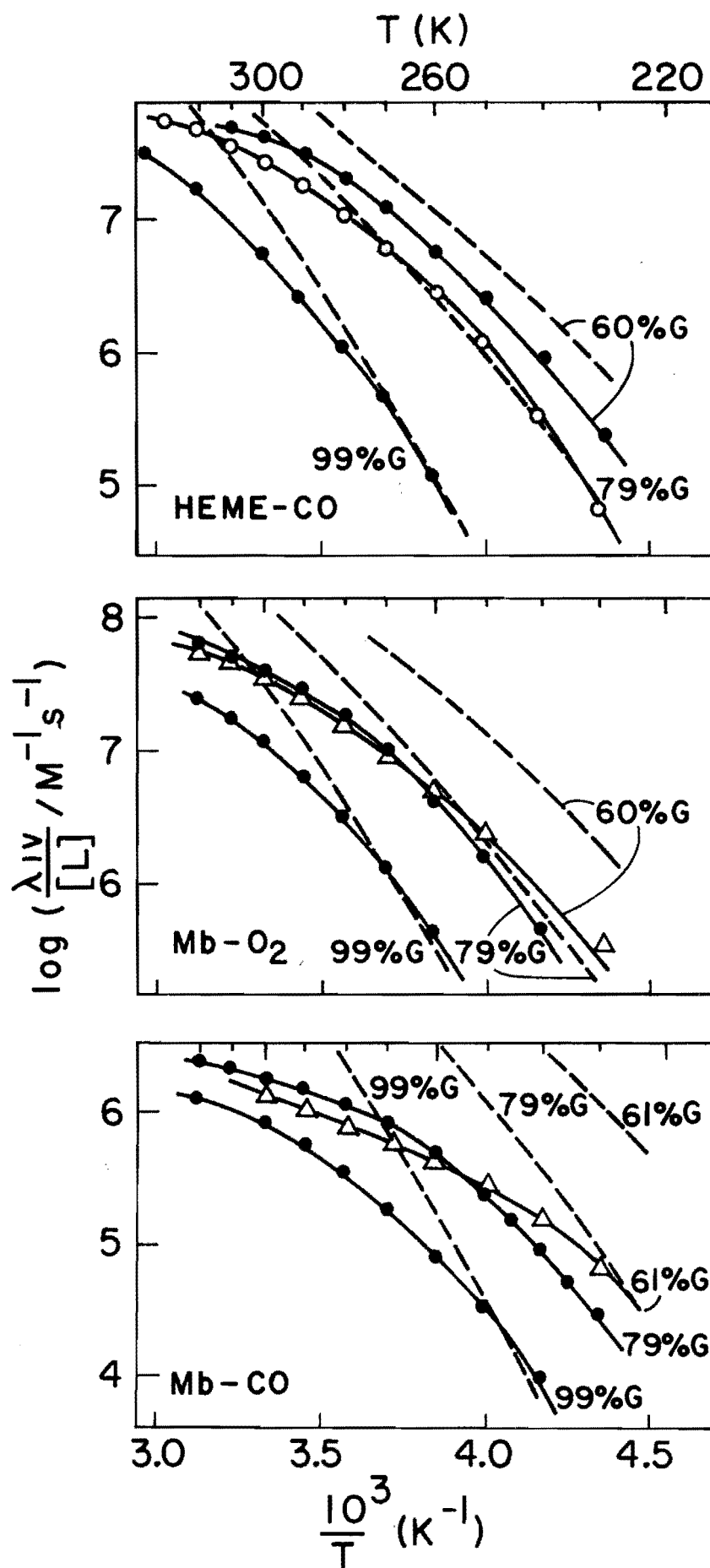
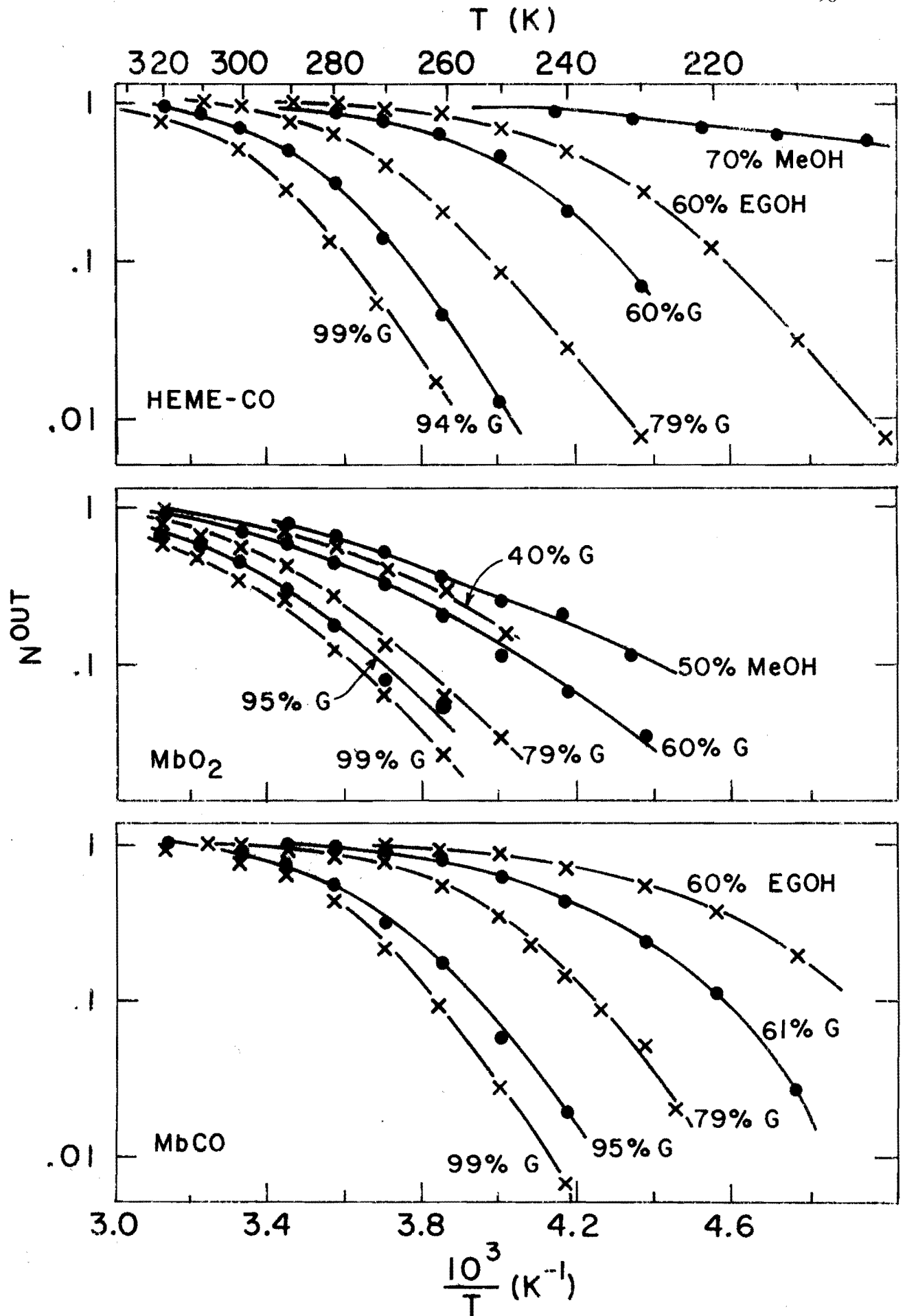


Figure 20

$N^{\text{out}}$ , the fraction of photodissociated ligands rebinding via process IV, versus  $1000/T$ . Fewer ligands are able to separate from the protein as the viscosity increases. The values are consistent with the criteria that  $N^{\text{out}}$  is small when the rates become diffusion controlled.



In order to apply Eigens criterion, one must choose the interface region within the multiple barrier model. The logical choice is the well adjacent to the solvent. One can then compare the diffusional separation rate  $k_{DS}$  to the overall binding rate from the interface region. This is shown in figure 21 and also implies that the diffusion controlled region is at low temperatures in the high viscosity solvents.

As a final criterion, one can compare the rates for various protein-ligand systems. If  $s$  is independent of the system, then one would expect a convergence of rates in the diffusion limited region. The results are shown in figure 22 and are consistent with the other criteria.

It is concluded that diffusion does play some role in the control of the rate of process IV in the low temperature, high viscosity region. This conclusion is in agreement with Hasinoff (Hasinoff, 1977), although his analysis is different. The value of  $s$  indicates that few collisions with a Mb molecule are successful towards binding. Less than 1% of the protein surface serves as a target for the ligands. This would support the concept of a well defined pathway for the ligand, as opposed to treating the Mb as a open structure with many entrances, as might be suggested when looking at only the backbone atoms of figure 1.

A diffusion model for protoheme-CO shall now be described. The step DA will still be considered a barrier requiring two parameters. The step SD will simply be the



Figure 21

A plot depicting Eigen's criteria for diffusion. The solid lines are the rates for the ligand to go over the last barrier toward the solvent. The dotted lines are the rates for the ligand to go from this interface region to the binding site. For protoheme-CO this rate is simply the single rate coefficient  $k_{DA}$ , which is independent of solvent. For the protein systems, the return from the interface region to the binding site involves more than one barrier. The dotted lines for Mb represent this overall rate, labeled  $\lambda_{III}$  for Mb-CO. When the rate to bind from the interface region is greater than the rate for the reactants to separate, the kinetics are said to be diffusion controlled. The rates become diffusion controlled at the low temperatures of the high viscosity solvents.

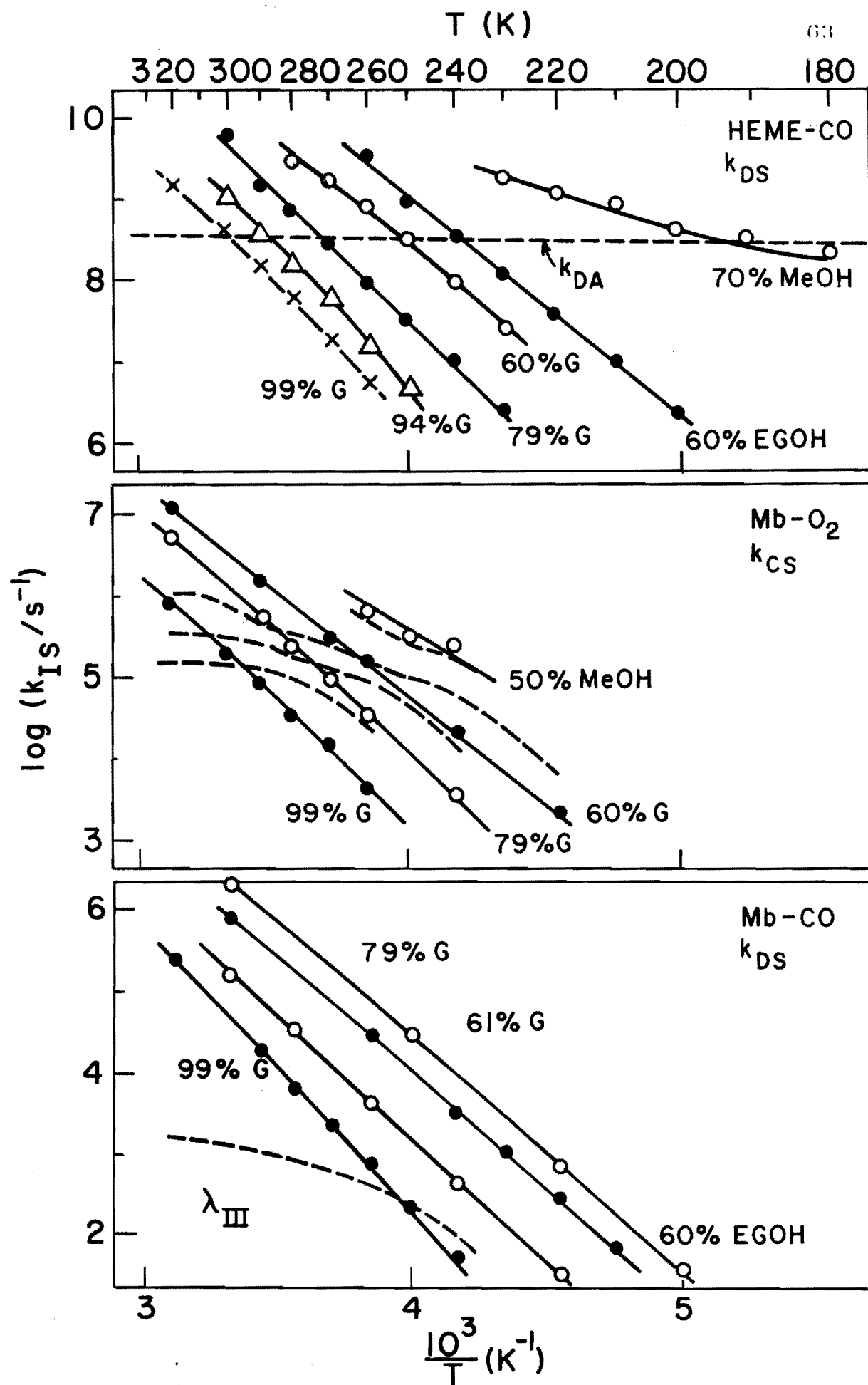
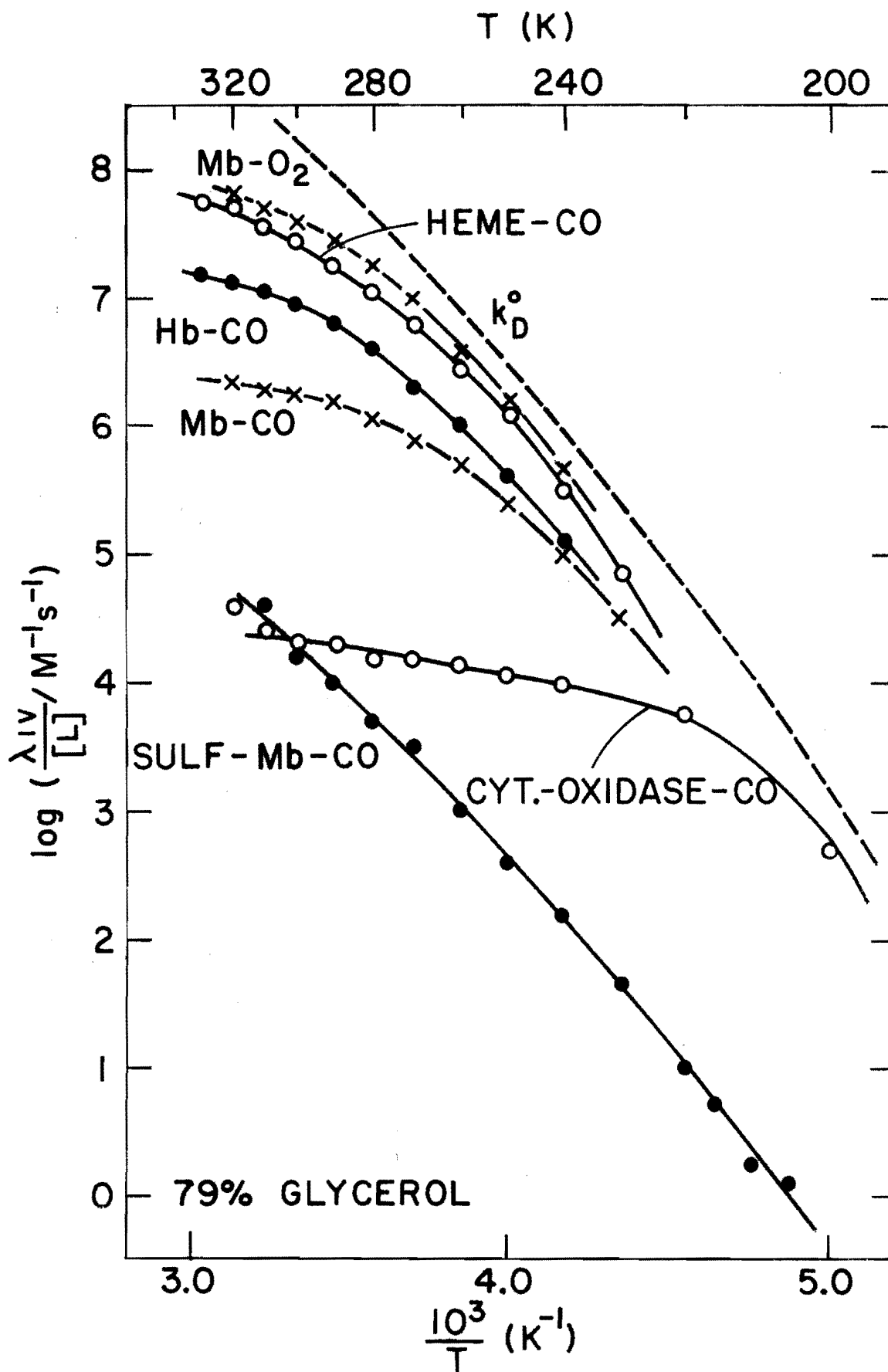


Figure 22

The rates for process IV versus  $1000/T$  for various protein ligand systems. The rates converge at low temperature indicating that the solvent is controlling the rate. The dotted line is the rate for diffusion limited kinetics (eq 12 with  $sr = .3A$ ). The rates for Sulf-Mb-CO do not depend on the solvent viscosity and is an example of a system that could be fit with a diffusion model (with extreme steric hindrance,  $s = 10^{-6}$ ), but fails other criteria for being diffusion controlled.



collision frequency (eq 12) with one free parameter. Well D is assumed to be a volume of solvent from where a ligand can jump to well A or out to the solvent. Rates from well D are now dependent the probability that a ligand is in well D ( $p_D$ ), and can be written as  $k_{DA}'' = p_D k_{DA}$ . The probability at equilibrium will depend on [CO] and the volume of well D ( $V_D$ ). When [CO]=1M, there are  $1600A^3$  per ligand. Thus  $p_D = V_D [CO] / 1600MA^3$ , which should be much less than one for typical values of [CO] = 300uM.

The rate  $k_{DS}$  (rate when  $p_D=1$ ) is expected to be the rate for a ligand to jump from one site in the solvent to another. If the average time between jumps is  $\tau$  and the average distance per jump is  $d$ , then the jumping rate  $k_j = 1/\tau = D_{CO}/d^2$ . Thus  $k_{DS} = \frac{1}{2} D_{CO}/d^2$ , the factor 1/2 accounting for the probability of the ligand jumping back to well D within a few steps. The factor is not necessarily 1/2, but depends on the relative probabilities of jumping to the solvent or to other sites in D. The three rate coefficients and four parameters for the diffusion model are:

$k_{DA}'' = p_D v \exp(S_{DA}/R) \exp(-H_{DA}/RT)$	$S_{DA}, H_{DA}$
$k_{SD} = k_{SD}' [CO] = s (7.57 \times 10^{21}) D_{CO} r [CO]$	$s$
$k_{DS}'' = p_D k_{DS} = (V_D [CO] / 1600MA^3) D_{CO} / d^2$	$V_D$

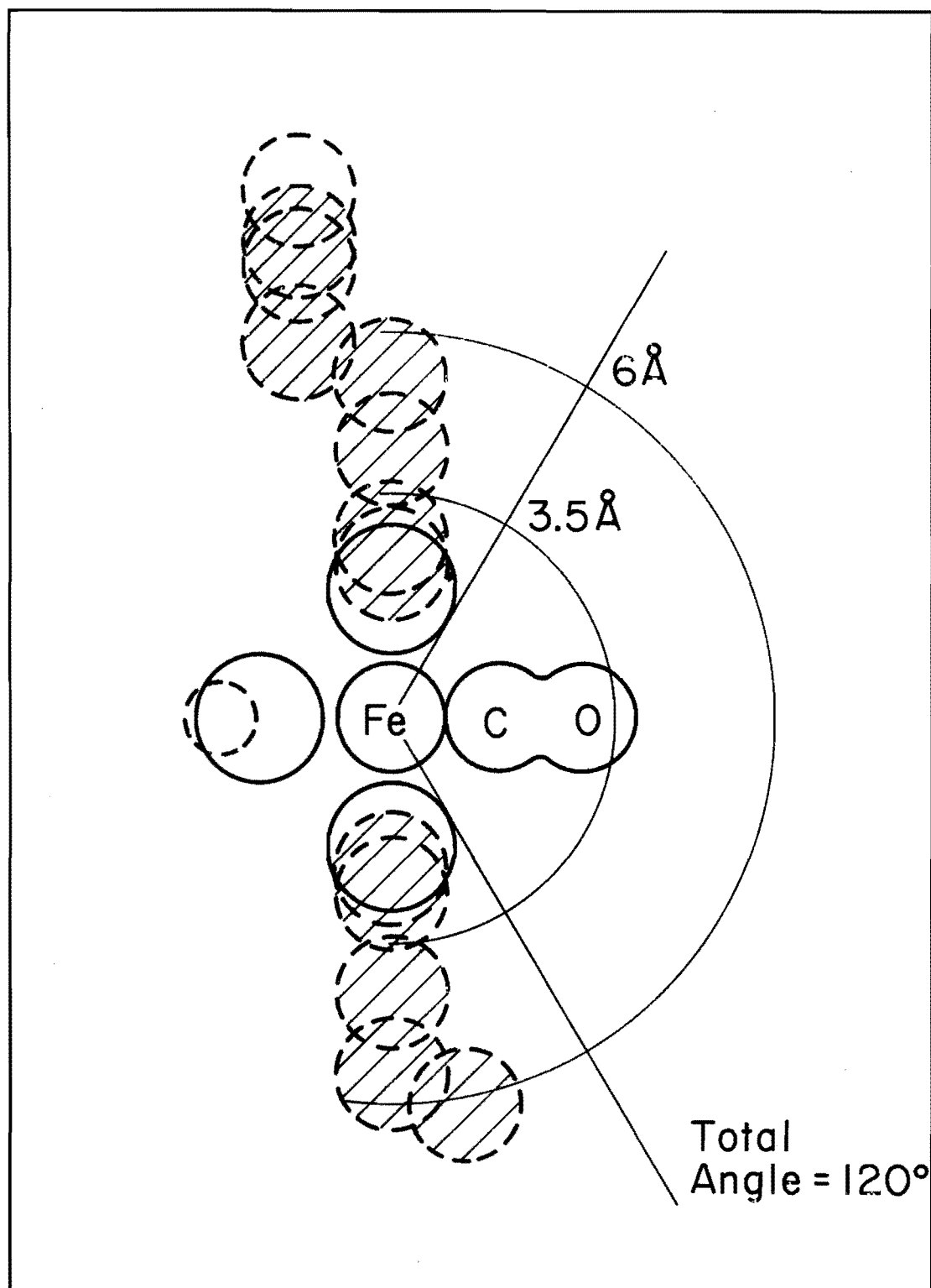
The kinetics consist of the following. The laser pulse takes the ligands from well A to D. The probability of the

ligand being in well D is temporarily 1. A certain fraction of the ligands will rebind directly with rate  $\lambda_I = k_{DA} + k_{DS}$ . The remaining fraction,  $N^{out} = k_{DS} / (k_{DA} + k_{DS})$ , will wander out to the solvent and compete with other CO molecules for binding sites. Now  $p_D < 1$  and the second rebinding process occurs at the rate  $\lambda_{IV} = k_{SD} * k_{DA} / (k_{DA} + k_{DS})$  which has two limiting forms. At high viscosity when  $k_{DA} \gg k_{DS}$ , the rates become diffusion controlled with  $\lambda_{IV} = k_{SD}$ . When  $k_{DA} \ll k_{DS}$ , the rate is  $\lambda_{IV} = (k_{SD} / k_{DS}) k_{DA} = p_D k_{DA}$ . The three observables to be fit are the rates of the two processes and the amplitude of the slow process.

The fast process is fit at low temperature where the kinetics were slow enough to measure ( $p_D = 1, \lambda_I = k_{DA}$ ). The amplitude of the slow process can be fit using values of  $k_{DA}$  extrapolated from low temperature and  $k_{DS}$  (since  $p_D = 1$ ; the best fit is when  $d = 2.2A$ ). This leaves the rate of the slow process which has two distinct regions. The rates at high viscosity can be simulated by the diffusion rate (eq 12) with  $sr = .3A$ , or  $s = .046$  when  $r = 6A$ . At high temperature, a value of  $p_D = [CO] / 6M$  will then complete the fitting of the kinetics. This value is equivalent to saying that  $p_D = 1$  when  $[CO] = 6M$ , which implies  $V = 260A^3$ . This is about 1/4 the volume between spheres of radii  $3.5A$  and  $6$  to  $7A$  (figure 24). With four parameters all the data can be fit, within a factor of two (which is less than the errors in the diffusivities and  $k_{DA}$ ). A similar model may be useful in describing the outer barrier of the Mb data.

Figure 23

A side view of protoheme (figure 1), showing half the atoms (the other half would be on an axis perpendicular to the page; Weissbluth, 1974). A water molecule is bound to the fifth position (left side) leaving the sixth position available for binding CO. The solid circles represent atoms in the plane of the page (N atoms above and below the Fe atom). The dotted circles are C or O above and/or below the plane. The iron is supposedly out of the heme plane by .1-.25A (toward the water when CO is not bound). Well D is estimated to be the volume between spheres of radii 3.5A and 6 to 7A constrained to a cone of total angle 120. This would satisfy the diffusion model calculations that the volume of well D is about  $260\text{\AA}^3$ , but does not have enough steric hindrance ( $s=.25$  here compared to .046 needed to fit the data). Possibly an additional factor of 1/2 in  $s$  is needed since the CO molecule may be facing in the wrong direction half the time; however, the rotational rate should be four times as large as the jump rates. A smaller angle of constraint would be required to give the observed steric hindrance.





## Appendix B: Nonexponential Kinetics

In the analysis section it was stated that the kinetics were fit with a multiple barrier model. There are a few subtle problems with fitting the type of kinetics seen in heme proteins. It can be seen in figure 7 that the kinetics for process I at low temperatures are not exponential. The data can be fit with a distribution of rates, as if each Mb has frozen slightly differently and has its own rate of recombination. At temperatures above 250K the kinetics have relaxed to a single rate (or else the kinetics of even the slower processes would be nonexponential). The question then arises: at what temperature does process I become exponential. And does it relax completely or only for times longer than some critical time.

Unfortunately process I cannot be seen in great detail at high temperature (figures 6 and 8). It appears that the kinetics relax around 260K for Mb-O<sub>2</sub>. Since the data are fit only in the region where all processes can be seen, it is important to treat process I properly. At temperatures such as 220K (figure 7) process I can still be fit well by extrapolating the results from fitting the low temperature region (60K-160K). Fitting with a single exponential results in a poor fit with some uncertainty in choosing the remaining parameters. Although the step BA can be thought of as

requiring only 2 parameters, it is often beneficial to use the low temperature results as a guide to the choice of these parameters. The fitting is certainly smoother using the extrapolation. Once process I is fit reasonably well, the remaining parameters for the other processes can be determined.

A second problem requires a closer look at the data at short times in figures 6 and 8. If the first process seen at each temperature is process I, then successively higher temperatures should be faster and therefore fall below the lower temperatures. Yet the results are the opposite, as if a new process emerges at each temperature. This might indicate that the ligand is able to wander slightly further away from the binding site as the temperature is raised. Certainly all of the wells and barriers are meant to represent an approximation to the real situation. Second order oscillations on the potential energy diagram are interesting, but were not incorporated in the fitting to keep the number of parameters to a minimum.

### Appendix C: Other proteins

One can question whether the results obtained are peculiar to Mb or are a general property of proteins. Several other heme proteins have been studied: Hb, cytochrome c, and P-450. They all show multiple barriers and are sensitive to the solvent viscosity. This again indicates that it is the biomolecule (with solvent influence) that governs the binding properties. In a completely different system, purple membrane, there is also a dependence on viscosity of the rates of its photocycle. Thus the fluctuations of biomolecules may be a general property necessary to perform some functions.

Different species of Mb and Hb have also been studied. The various species of Mb differ by 5 to 25 of the 153 amino acids. It was hoped that the results might help determine the location of the barriers. Although the kinetics of several species are distinguishable at both high and low temperatures (figures 24 and 25), few conclusions can be drawn as to which amino acids are responsible. The different species show a similar dependence on viscosity. The results do show that changes in the protein structure can effect the kinetics.

One can also attempt to change the structure of the protein by adding certain detergents which are known to cause Mb to unfold. Adding small amounts of such detergents could cause a slightly different tertiary structure. Dodecyl sodium

Figure 24

The kinetics for three species of Mb in 79% glycerol. (●=sperm whale, ○=dwarf sperm whale, □=harbor seal). The dwarf and sperm whales differ by 5 of the 153 amino acids. Results for horse, common porpoise, common dolphin, and california sea lion are similar to those of the harbor seal.

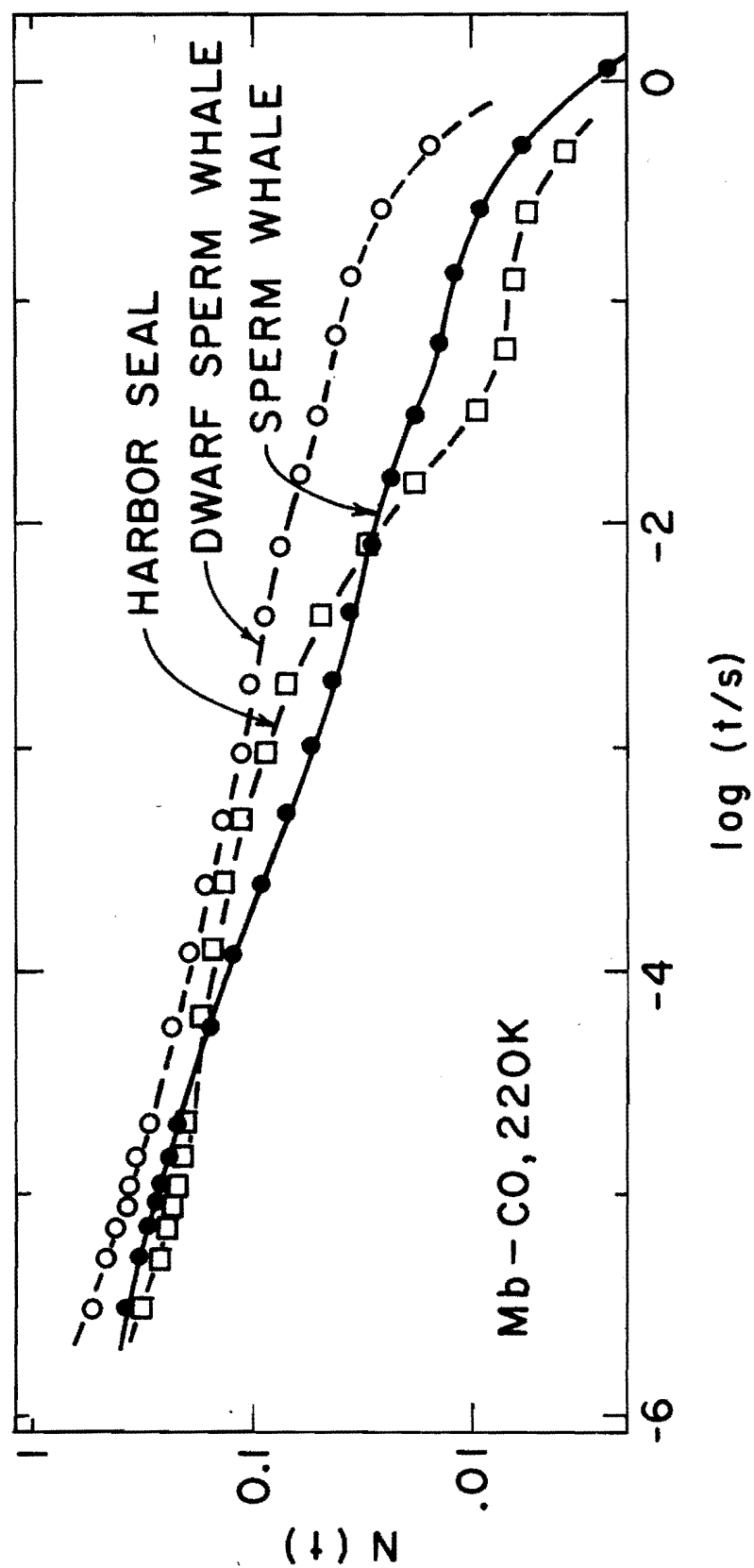


Figure 25

Low temperature kinetics for the same three species (symbols as in figure 24). Apparently the distribution of rates is sensitive to small changes in the overall Mb structure. Results for various species of tetrameric hemoglobin show larger differences.

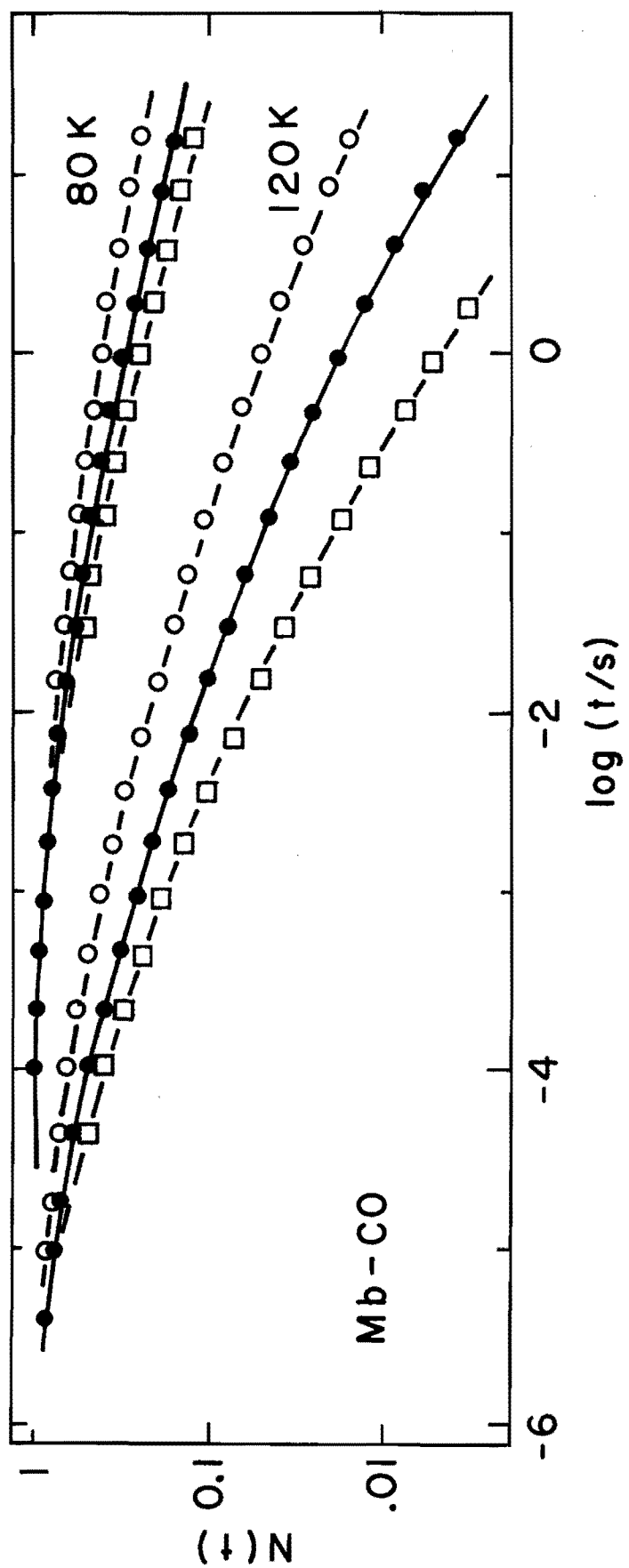


Figure 26

Kinetics for Mb-CO in 79% glycerol with and without the detergent dodecyl-sodium-sulfate (SDS). Sufficient amounts of SDS will cause the protein to unfold. A ratio of 5 SDS to 1 Mb was used here, causing less than a 5% decrease in the visible spectrum of the Mb-CO.



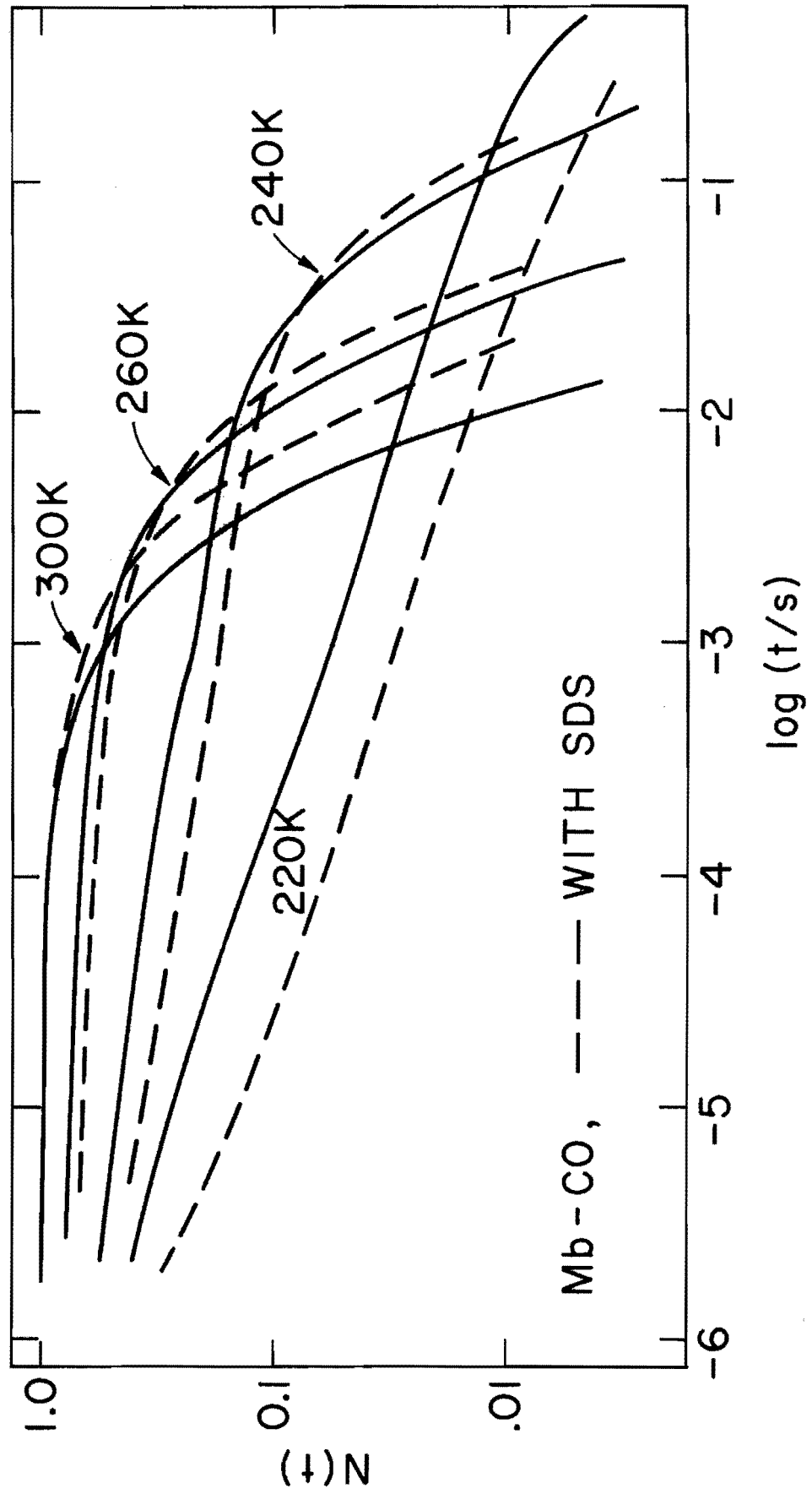
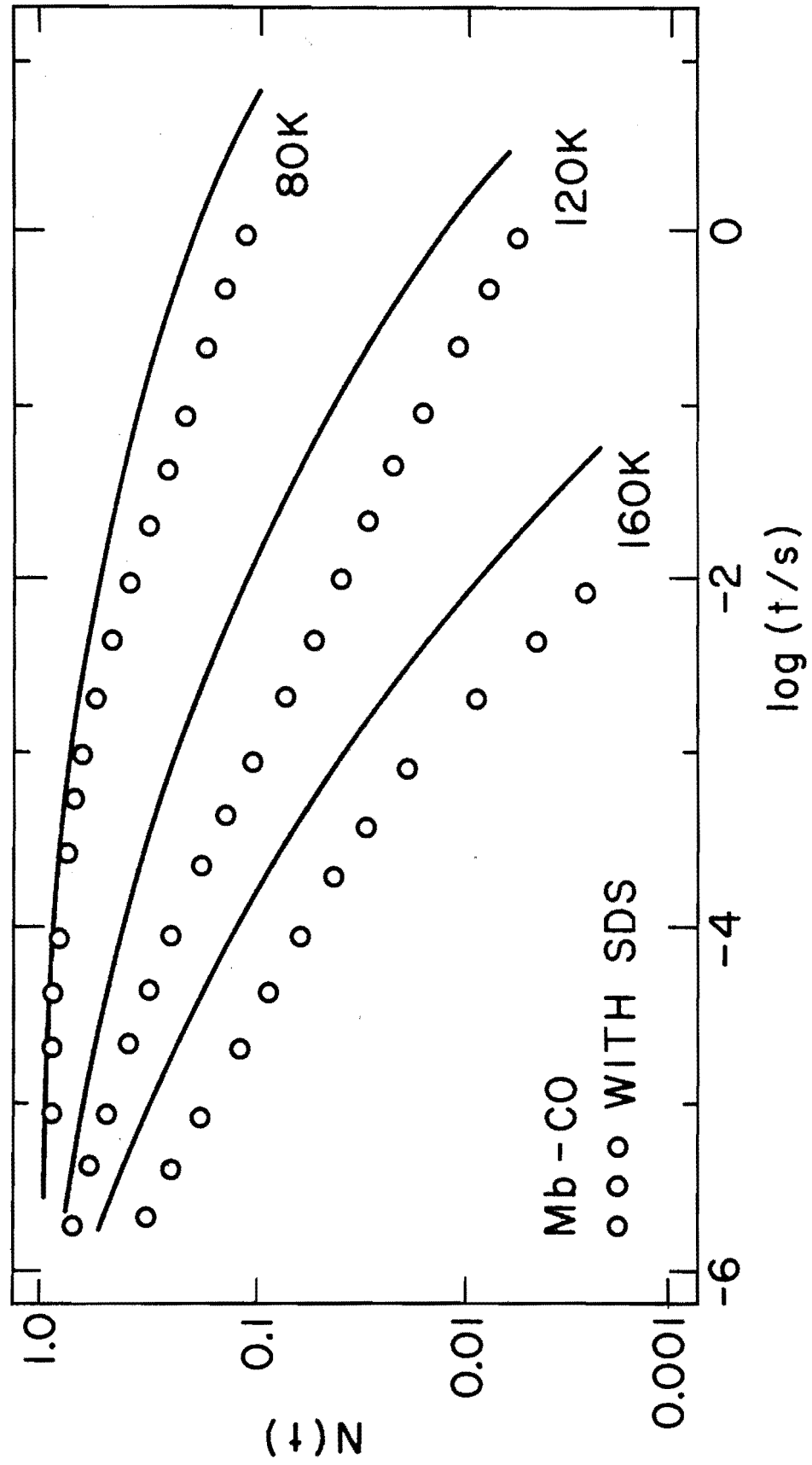


Figure 27

Low temperature results for Mb-CO with and without dodecyl sodium sulfate (SDS). Small amounts of the detergent caused process I to become faster. This is in the direction toward the kinetics of protoheme, indicating the heme group may now have more room.



sulfate (SDS) was added to Mb-CO in 79% glycerol. The rates at low temperature were then faster and the barriers were slightly changed (figures 27 and 28).

The kinetics of heme proteins are dependent on the protein structure and are sensitive to small changes in the protein and its environment. The barriers do not seem to be static, but are a result of fluctuations of the protein. At biological temperatures the kinetics are governed by the protein structure rather than diffusion; however, the rates do depend on the viscosity of the protein environment.

## REFERENCES

- Abras, A. and J.G. Mullen (1972) Phys. Rev. A 6, 2343.
- Ackerman, E. and R.L. Berger (1963) Biophysical J. 3, 493.
- Alberding, N., S.S. Chan, L. Eisenstein, H. Frauenfelder, I.C. Gunsalus, and T.M. Nordlund (1976) J. Chem. Phys. 65, 4701.
- Antonini, E. and M. Brunori (1971) Hemoglobin and Myoglobin in Their Reactions with Ligands, North-Holland Publishing Co., Amsterdam.
- Austin, R.H., K.W. Beeson, L. Eisenstein, H. Frauenfelder, and I.C. Gunsalus (1975) Biochemistry 14, 5355.
- Beece, D. L. Eisenstein, H. Frauenfelder, D. Good, M.C. Marden, L. Reinisch, A.H. Reynolds, L.B. Sorensen, and K.T. Yue (1980) Biochemistry (in press).
- Blomberg, C. (1977) Physica 86, 49.
- Brinkman, H.C. (1956) Physica 22, 149.
- Case, D.A. and M. Karplus (1979) J. Mol. Biol. 132, 343.
- Chandrasekar, S. (1943) Rev. Mod. Phys. 15, 1.
- Cooper, A. (1976) Proc. Natl. Acad. Sci. USA 73, 2740.
- Craig, P.P. and N. Sutin (1963) Phys. Rev. Lett. 11, 460.
- Dickerson, R.E. (1964) The Proteins Vol 2, H. Neurath ed., p603, Academic Press, New York.
- Douzou, P. (1977) Cryobiochemistry, London, Academic Press.
- Eigen, M. (1974) in Quantum Statistical Mechanics in the Natural Sciences, Plenum Press, New York.
- Frauenfelder, H., G. Petsko, and D. Tsernoglou (1979) Nature 280, 558.
- Glasstone, S., K.J. Laidler, and H. Eyring (1941) The theory of rate processes, McGraw Hill, New York.

- Hasinoff, B.B. (1977) Arch. Biochem. Biophys. 183, 176.
- Jordan, J., E. Ackerman, and R.L. Berger (1956) J. Am. Chem. Soc. 78, 2979.
- Kirkwood, J.G. (1946) J. Chem. Phys. 14, 180.
- Kramers, H.A. (1940) Physica 7, 284.
- Kubo, R. (1966) Rep. Prog. Phys. 29, 255.
- Miner, C.S. and Dalton, N.N. ed. (1953) Glycerol, Reinhold, New York.
- Reif, F. (1965) Fundamentals of statistical and thermal physics, McGraw-Hill, New York.
- Seidell, D. (1940) Solubilities Vol. I., D Van Nostrand, New York.
- Smoluchowski, M. (1916) Physk. Zeits. 17, 557.  
(1917) Z. Physik. Chem. 92, 129.
- Vaughan, W.M., and G. Weber (1970) Biochemistry 9, 464.
- Weissbluth, M. (1974) Hemoglobin: Cooperativity and Electronic Properties, Springer-Verlag, New York.

## VITA

Born: August 12, 1953 in Elmhurst, Illinois.

Education: University of Missouri - Rolla, BS-Physics Dec, 1974.  
University of Illinois - Urbana, MS-Physics May, 1976.

Coauthor of the following publications:

Fast Reactions in Carbon Monoxide Binding to Heme Proteins  
Biophys. J. 24, 319 (1978)

Dioxygen Replacement Reaction in Myoglobin  
Biochemistry 18, 3421 (1979)

Solvent Viscosity and Protein Dynamics  
Biochemistry (1980)

Solvent Viscosity and the Dynamics of Dioxygen Binding to  
Myoglobin, "Interaction between Iron and Proteins in  
Oxygen and Electron Transport", ed. Chien Ho, Elsevier  
North Holland Inc., New York, NY (1980)

The Effect of Viscosity on the Photocycle of Bacteriophodopsin  
Photochem. and Photobiol. (1980)

Isotope Effect in Molecular Tunneling  
Phys. Rev. Letters 44, 1157 (1980)